

Design and Manufacturing of a Miniature Turbojet Engine

A Major Qualifying Project
Submitted to the Faculty of
WORCESTER POLYTECHNIC INSTITUTE
in partial fulfillment of the requirements for the
Degree of Bachelor of Science



Submitted by:

Daniel Alonzo
Alex Crocker
Eric James
John Kingston III

Submitted on: March 23, 2018

Submitted to:

Project Advisor: Robert Daniello, WPI

Abstract

The goal of this major qualifying project was to design and manufacture a small gas turbine engine. The manufactured components included: axial turbine, stator, diffuser, compressor inlet, shaft, outer casing, combustion chamber, fuel distributor, exhaust nozzle, and inlet flange. We reviewed literature regarding gas turbine engine components, designed each component, and manufactured them accordingly. We then assembled our engine and planned for testing.

Acknowledgements

Our team would like to take this moment to thank the many people who contributed to the success of our project.

We would like to thank Capture 3D in South Windsor, Connecticut for helping us scan our compressor wheel.

We would like to thank Henke Sass Wolf in Dudley, Massachusetts for helping us laser weld our fuel distributor and donating material used for our combustion chamber.

We would like to thank Peterson Steel in Worcester, Massachusetts for donating material used for the stator, stator housing, diffuser, turbine, and inlet shroud.

We would like to thank the staff of Washburn shops for assisting us throughout the manufacturing process.

Finally, we would like to thank our advisor, Professor Robert Daniello, for always pushing us to do better, his continuous support and encouragement, and his overall commitment to the success of our project.

Table of Contents

ABSTRACT	II
ACKNOWLEDGEMENTS	III
TABLE OF CONTENTS	IV
TABLE OF FIGURES	VI
TABLE OF EQUATIONS	VII
TABLE OF TABLES	VIII
1.0 INTRODUCTION	9
2.0 BACKGROUND	12
2.1 Gas Turbines	12
2.2 Components	14
2.2.A. Compressor	14
2.2.B. Diffuser	18
2.2.C. Turbine & Stator	18
2.2.D. Combustion Chamber	23
2.2.E. Exhaust Nozzle	25
2.2.F. Fuel System, Lubrication & Bearings	27
2.3 Ideal Cycle Analysis	30
2.3.A. The Brayton Cycle	30
2.3.B. Ideal Component Analysis	33
3.0 METHODOLOGY	37
3.1 Compressor	37
3.2 Inlet Shroud	39

3.3 Diffuser	41
3.4 Combustion Chamber	43
3.5 Shaft Housing	44
3.6 Fuel Distributer	46
3.7 Turbine	47
3.8 Outer Casing & Inlet Flange	50
3.9 Shaft	53
3.10 Stator & Stator Housing	55
3.11 Exhaust Nozzle	56
3.12 Bearings, Fuel Injection, and Lubrication	58
4.0 CONCLUSIONS AND RECOMMENDATIONS	60
REFERENCES	63
APPENDIX A: IDEAL CYCLE ANALYSIS	65
APPENDIX B: TURBINE BLADE STRESS	70
APPENDIX C: FUEL CONSUMPTION CALCULATION	71
APPENDIX D: CAD DRAWINGS	72

Table of Figures

FIGURE 1: FOUR TYPES OF GAS TURBINE ENGINES (AVIATION, 2015)	14
FIGURE 2: EXAMPLE OF CENTRIFUGAL COMPRESSOR	15
FIGURE 3: COMPRESSOR MAP EXAMPLE (GARRET, 2017)	17
FIGURE 4: TURBINE WHEEL (LEFT) AND STATOR (RIGHT) EXAMPLES	20
FIGURE 5: VELOCITY VECTORS FOR STATOR AND TURBINE (MATTINGLY, 2000)	21
FIGURE 6: EXAMPLE OF AN ANNULAR COMBUSTION CHAMBER	24
FIGURE 7: EXAMPLE GEOMETRY OF OPEN BRAYTON CYCLE (FLACK, 2005)	31
FIGURE 8: T-V, P-V AND T-S DIAGRAMS (MIT, 2014)	32
FIGURE 9: GT4202 COMPRESSOR MAP (LIMIT ENGINEERING, 2015)	38
FIGURE 10: G4202 ATTACHED TO DRIVE SHAFT	39
FIGURE 11: INLET SHROUD	41
FIGURE 12: CHANNEL DIFFUSER	42
FIGURE 13: COMBUSTION CHAMBER	44
FIGURE 14: SHAFT HOUSING	45
FIGURE 15: FUEL DISTRIBUTOR	47
FIGURE 16: AXIAL TURBINE	50
FIGURE 17: OUTER CASING	51
FIGURE 18: INLET FLANGE	52
FIGURE 19: SHAFT ASSEMBLY	54
FIGURE 20: NOZZLE	57
FIGURE 21: LUBRICATION SYSTEM	59
FIGURE 22: NOZZLE (LEFT) AND COMPRESSOR (RIGHT) VIEWS OF ASSEMBLY	62

Table of Equations

EQUATION 1: PRESSURE RATIO ACROSS COMPRESSOR	15
EQUATION 2: CHANGE IN ENTHALPY ACROSS COMPRESSOR (KAMPS, 2005)	16
EQUATION 3: POWER INPUT FOR COMPRESSOR (KAMPS, 2005)	16
EQUATION 4: THRUST VECTOR (SHRECKLING, 1992)	21
EQUATION 5: CENTRIFUGAL FORCE CALCULATION (NPOWER, 2009)	22
EQUATION 6: BLADE ROOT NOMINAL STRESS	22
EQUATION 7: THERMAL OUTPUT EQUATION (SHRECKLING, 1992)	28
EQUATION 8: FUEL FLOW REQUIRED (SHRECKLING, 1992)	29
EQUATION 9: PRESSURE RATIO ACROSS INLET	33
EQUATION 10: TEMPERATURE RATIO ACROSS INLET	33
EQUATION 11: PRESSURE RATIO ACROSS COMPRESSOR	34
EQUATION 12: TEMPERATURE RATIO ACROSS COMPRESSOR	34
EQUATION 13: COMPRESSOR T-P RELATION (NASA, COMPRESSOR THERMODYNAMICS, 2015B)	34
EQUATION 14: COMPRESSOR WORK (NASA, COMPRESSOR THERMODYNAMICS, 2015B)	35
EQUATION 15: PRESSURE RATIO ACROSS COMBUSTOR	35
EQUATION 16: PRESSURE RATIO ACROSS COMBUSTOR	35
EQUATION 17: PRESSURE RATIO ACROSS TURBINE	36
EQUATION 18: TEMPERATURE RATIO ACROSS TURBINE	36
EQUATION 19: TURBINE T-P RELATION (NASA, TURBINE THERMODYNAMICS, 2015D)	36
EQUATION 20: TURBINE WORK (NASA, TURBINE THERMODYNAMICS, 2015D)	36
EQUATION 21: PRESSURE RATIO ACROSS NOZZLE	36
EQUATION 22: TEMPERATURE RATIO ACROSS NOZZLE	36

Table of Tables

TABLE 1: SPECIFIC ENERGY AND DENSITY OF DIFFERENT FUELS.....	27
TABLE 2: STAGES OF GAS TURBINE ENGINE	31

1.0 Introduction

The gas turbine engine is a machine that, according to the thermodynamic Brayton Cycle, does work by harnessing energy from a working fluid and converting the energy into a useable form. Various types of gas turbines are designed to perform a range of tasks but all operate on similar principles. Air enters the engine, is compressed, mixed with fuel, combusted, and then expanded through a rotating turbine. Common applications of modern gas turbines include: producing auxiliary power for ground or aircraft systems, propelling military aircraft at supersonic speeds, and driving the rotor system of helicopters (Macisaac & Langton, 2011). Due to the extreme temperatures and high rotational speeds experienced by engine components, design and construction of a gas turbine demands accuracy, informed material selection, knowledge of thermodynamics, and the ability to model and machine metal components.

As material processing techniques advanced, it became possible to manufacture gas turbine engines small enough to power radio controlled (RC) airplanes. Modern gas turbines for full size aircraft generally utilize axial compressors and turbines with multiple stages of blades. These multi-stage components increase efficiency, pressure ratios, and performance characteristics (Shreckling, 1992). However, RC jet modelers found that small engines can be reasonably efficient and powerful with single stage compressor and turbine stages. A centrifugal compressor matched to an axial turbine has become a common design among RC jet enthusiasts. With this simplification, along with advancements in CNC machining and 3D modeling, it is possible to manufacture a complete miniature gas turbine with a relatively small investment.

Although miniature gas turbines are now available for sale from a number of manufacturers, the secrets of design and construction are still somewhat hidden from the end customer. Accurate analysis of performance is elusive even with the utilization of modern software, and an iterative design process offers the soundest path toward new engine development (Stricker, 1998). However, a number of publications are available that instruct the ambitious RC jet enthusiast on how to manufacture an engine with amateur means.

The goal of this project is to call on the literature available regarding small gas turbines in order to design and manufacture an engine that is self-sustaining. In order to expedite the design process, efficiency and thrust production are not prioritized. Due to budget and time restrictions we are unable to complete multiple iterations of a new engine. Therefore, we rely on engine designs currently developed to aid in the design of our major components. Subjects such as new airfoil design for turbine blades, nozzle efficiency, and combustor efficiency can be the subject of years of research and investment. For this reason, we drew on industry standards and recommendations of modelers to design some of our components. We realized early that two crucial components, the centrifugal compressor and ball bearings, would be impossible to design and manufacture given the time frame. We made the decision to purchase these components in order to make our project more feasible given the restrictions.

This project culminated in the manufacture of twelve major components.

- Compressor inlet shroud
- Diffuser
- Power transmitting shaft
- Shaft housing
- Annular Combustion chamber

- Fuel distributor
- Stator
- Stator/turbine housing
- Axial Turbine
- Exhaust nozzle
- Outer casing
- Inlet flange

Additionally, we assembled our components and added a fuel injection system and bearing lubrication system. Due to time constraint, we were unable to implement a throttle mechanism or construct a simple and safe engine stand and were not able to test the engine. Each component listed above was first modeled with SOLIDWORKS software and then manufactured with the material processing capabilities available in Worcester Polytechnic Institute's Washburn and Higgins Labs. Throughout the experience, our team furthered our design and manufacturing skills through manual and CNC milling and turning, TIG welding, sheet metal forming, and regular engineering troubleshooting.

2.0 Background

This chapter reviews previous research on gas turbines with an emphasis on small/miniature sized turbojets. We provide an introduction to gas turbines and their use as well as methods for conducting theoretical cycle analysis. Additionally, we introduce the components that constitute a modern small gas turbine.

2.1 Gas Turbines

A gas turbine is a type of continuous, internal combustion engine that contains three major components: a compressor, a combustor, and a turbine. A basic configuration, referred to as the turbojet, consists of an inlet nozzle where air at free stream velocity is directed into a compressor (Hunecke, 1997). The air is accelerated and compressed across the compressor stage and then redirected into the combustion chamber. Fuel is injected into the chamber, combined with the high-pressure air, and ignited to create combustion. The hot gas, which has expanded in the combustion chamber, is forced through the turbine blades resulting in rotation of the shaft which ties the turbine to compressor. From here the exhaust gas is accelerated through an outlet nozzle. The high velocity exhaust is at a speed much greater than the free stream velocity and therefore produces thrust.

The basis for the creation of thrust is Isaac Newton's second law of motion, force is equivalent to mass times acceleration (Shreckling, 1992). According to the principles of conservation of momentum, the thrust force created by the turbojet is equal to the mass flow rate of the exhaust gas multiplied by the velocity relative to the free stream velocity of air entering the compressor. The more fuel that is consumed by the engine, the more

thrust is created, assuming constant efficiency. One method for increasing the amount of thrust is by afterburning, also known as thrust augmentation. This design incorporates a separate burner that combusts extra fuel and releases hot exhaust gases downstream from the turbine (Britannica, 2018). Afterburners can substantially increase thrust at the expense of rapid fuel consumption. However, afterburners are primarily used in military aircraft to achieve supersonic flight.

Some gas turbines do not generate thrust and instead have become a popular method for power generation due to increases in efficiencies (Boyce, Meherwan P., et al., 2012). Although these industrial applications for gas turbines exist, this paper focuses on aircraft propulsion applications. Four main types of turbines utilized in the aerospace industry are the turbojet, turbofan, turboprop and turboshaft.

Turbojet and turbofan engines provide thrust generated from reaction forces created by high velocity exhaust gas leaving the outlet nozzle. The turbofan is the most common type of engine used in the aerospace industry (Hunecke, 1997). It utilizes a fan that is upstream the compressor, which is also driven by the turbine. Air bypasses the compressor and rejoins the flow downstream of the turbine adding “cold thrust.” This design achieves better fuel efficiency than turbojet engines while operating at cruising speeds common to civil airline travel. The turbojet engine, unlike the turbofan, does not allow air to bypass the compressor, it is simple by design and the earliest type of turbine propulsion engine.

Turboprop and turboshaft engines use exhaust gases to drive a separate turbine that drives a propeller. The difference between the two is that the turboshaft utilizes all exhaust gas to drive the propeller, whereas the turboprop also uses some of this exhaust

gas to produce thrust. Turboshaft engines are commonly used in helicopters, such as the Sikorsky CH-53G. Figure 1 below gives a visual representation of these four engines.

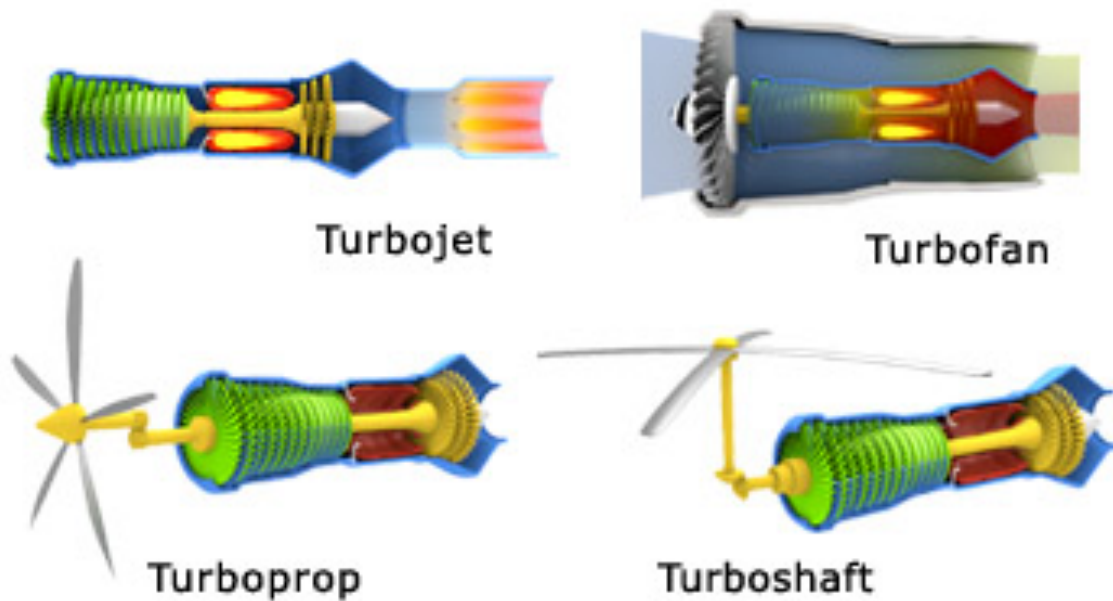


Figure 1: Four Types of Gas Turbine Engines (Aviation, 2015)

2.2 Components

In order to better understand how a small turbojet engine operates, one must understand the purpose for each component. This section reviews the conceptual physics and thermodynamics as they relate to each individual component.

2.2.A. Compressor

As we now know, the compressor is the stage of the engine which creates high enough pressure to achieve combustion. The two types of compressors commonly used in

turbojet engines are axial and centrifugal (Stricker, 1998). The axial compressor directs the air flow parallel to the rotational axis whereas the centrifugal design directs the flow radially outward, perpendicular to the rotational axis. Small gas turbines, that produce less than 5 MW, are often designed around centrifugal compressors. Although these are less efficient than multi-stage axial compressors, centrifugal compressors are reliable and able to produce pressure ratios in excess of 8:1 with a single stage (Kamps, 2005). The pressure ratio is equal to the total pressure downstream the compressor divided by the pressure at the compressor entry.

$$\Pi = \frac{P_2}{P_1}$$

Equation 1: Pressure Ratio Across Compressor

This ratio impacts thrust, fuel consumption and engine efficiency. An example of a centrifugal compressor can be seen in Figure 2.

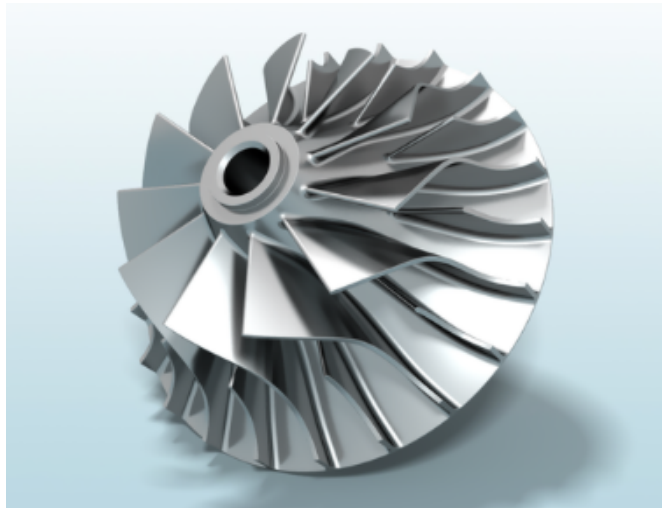


Figure 2: Example of Centrifugal Compressor

Regardless of the exact geometry in the centrifugal compressor, the purpose is to redirect the air radially along the axis of rotation (NASA, Compressor, 2015a). Air flows along the blades of the compressor and is sent out in the radial direction by centrifugal force. The high-speed air accelerated by the compressor then enters the diffuser stage of the engine. The increase in pressure across the compressor is accompanied by increases in temperature and enthalpy (Kamps, 2005). Change in enthalpy across an adiabatic compressor can be defined by:

$$\Delta h = TC_p(\pi^{0.286} - 1)$$

Equation 2: Change in Enthalpy Across Compressor (Kamps, 2005)

where,

$$\Delta h = \text{Change in Enthalpy} \left(\frac{J}{kg} \right)$$

$$T = \text{Inlet temperature of air (Kelvin)}$$

$$C_p = \text{Specific heat of air entering compressor} \left(\frac{KJ}{KgK} \right)$$

$$\pi = \text{Pressure ratio of the compressor}$$

This rise in enthalpy is proportional to the input power provided by the turbine to the compressor, which can be seen in the following expression.

$$P = \frac{\dot{m}\Delta h}{\eta}$$

Equation 3: Power Input for Compressor (Kamps, 2005)

where,

$$\Delta h = \text{Enthalpy increase } \left(\frac{J}{kg} \right)$$

$$P = \text{Power input (W)}$$

$$\eta = \text{Efficiency}$$

$$\dot{m} = \text{Mass flow of air through compressor } \left(\frac{kg}{s} \right)$$

From empirical data and computer simulation, performance of a compressor can be represented by compressor maps. These charts plot performance characteristics of a compressor in order to understand the compressors' capabilities. Typically, mass flow rate and pressure ratio are plotted, although sometimes rotations per minute (RPM) or efficiency are seen. An example of a standard compressor map can be seen below in Figure 3.

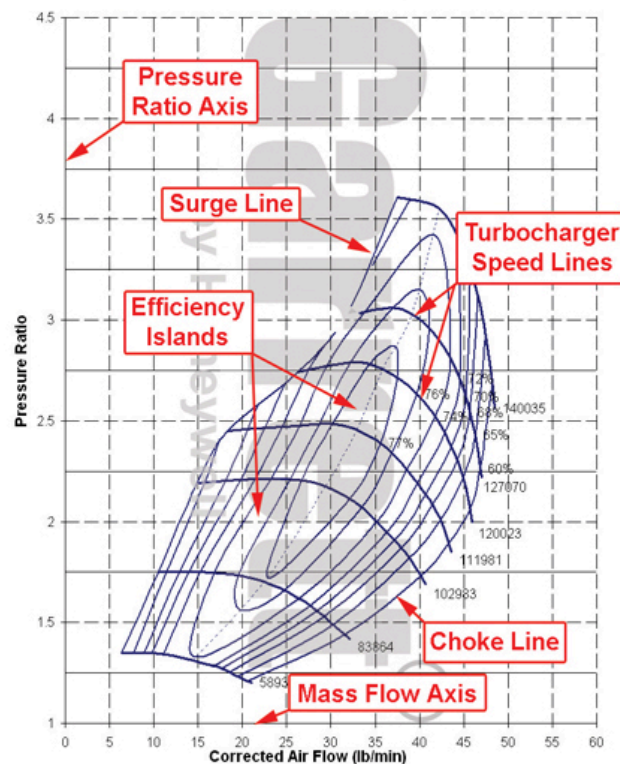


Figure 3: Compressor Map Example (Garret, 2017)

2.2.B. Diffuser

The purpose of a diffuser is to decelerate the speed of the incoming compressed fluid, converting the speed of the gas into pressure. Essentially, the diffuser converts high speed air in the form of kinetic energy into potential energy in the form of high pressure. There are a variety of acceptable diffuser designs for small gas turbines. One design, the radial wedged diffuser, has become popular among manufacturers of small gas turbines for model aircraft. The KJ66, a primitive engine design widely popular among RC jet enthusiasts, utilizes the radial wedged diffuser design (Ling, Wong, & Armfield, 2007). The blade configuration of these diffusers can vary greatly and still perform adequately, some are curved in the direction of rotation of the impeller while others curve in the opposite direction. However, perhaps the most desirable blade design characteristic for small gas turbines is that the blade widens to provide sufficient surface area for bolt holes (Kamps, 2005). These bolt holes provide a convenient location that allows the manufacturer to bolt the diffuser, compressor and inlet shroud into a ridged body.

2.2.C. Turbine & Stator

Turbines, like compressors, are designed as either axial or radial. Axial-flow turbines are the most widely used because they offer the possibility for higher mass flow rates than that of radial turbines. Typically, axial-flow turbines consist of multiple stages in order to increase efficiency and thrust production. However, when designing small gas turbines single stage axial turbines are often used. The turbine stage usually consists of nozzle stationary guide vanes, also known as a stator. Stator blades are airfoils with their

leading edges facing the combustion chamber (Hunecke, 1997). Their purpose is to reduce the phenomena known as swirl and allow air to accelerate into the turbine blades. The stator directs exhaust gases in the axial direction towards the turbine blades while increasing the absolute velocity and kinetic energy of the exhaust gases. The stator has a similar yet opposite role to that of the diffuser in the compressor stage. In the diffuser, the area between the adjacent blades increase in the downstream direction whereas in the stator this area increases.

The stator and turbine must contend with extremely high thermal loads. By raising the turbine inlet temperature, more thrust per unit mass flow rate is generated (Mattingly, 2000). The turbine also operates at extremely high angular velocities. These criteria have driven the development of new materials and cooling techniques used in this stage of the engine. Even small turbine blades can encounter exhaust gases with temperatures in excess of 1000 degrees centigrade while rotating upwards of 100,000 RPM. Due to high pressures, temperatures, and peripheral blade speeds nickel-based super alloys are often used (Mukinutalapati, 2011). These materials must also have high resistance of creep due to their continuous use under these conditions. Various companies have developed Nickel-Chromium super alloys for use in turbine blades. Common trade names for these alloys include: Inconel 625, Altemp 625, and Chronin 625. Examples of a turbine and a stator with housing can be seen in 5.

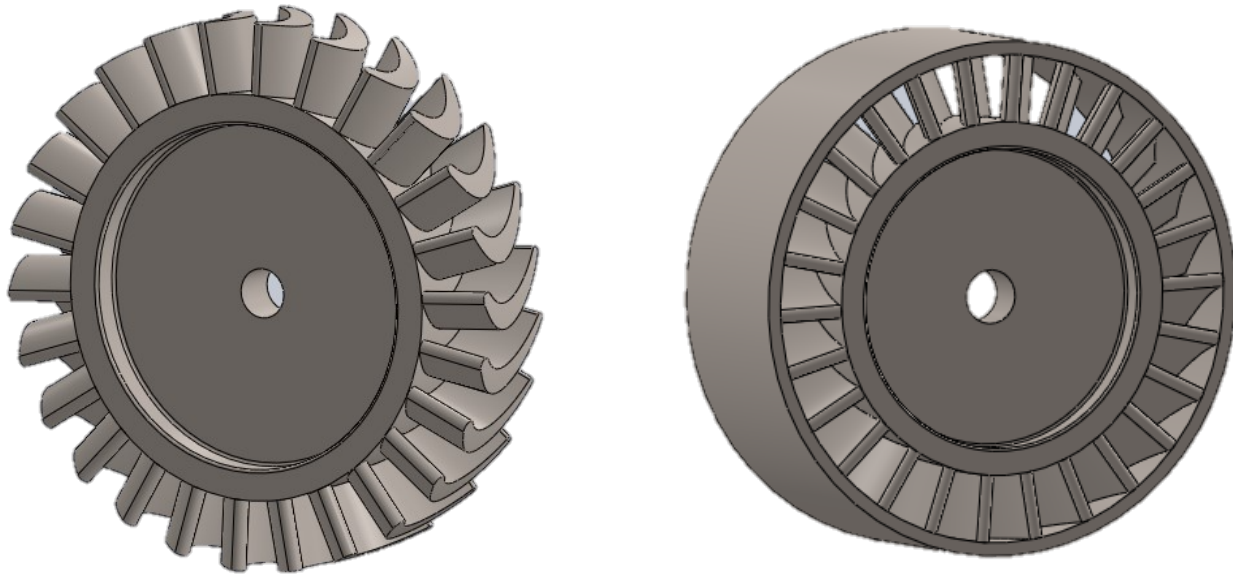


Figure 4: Turbine Wheel (left) and Stator (right) Examples

Turbine blade design is perhaps the most critical consideration for improving thrust creation. The goal in turbine blade design is to produce a velocity vector at the turbine exit that is the same magnitude and direction everywhere along the blade (Mattingly, 2000). The purpose of this design is to provide axially directed flow at turbine exit with as little swirl as possible, considering swirl is unusable for thrust creation. In order to better understand stator and turbine blade design it is necessary to examine vector analysis with velocity triangles.

Three standardized variables are commonly used in velocity diagrams to represent the interaction between the turbine blades and working fluid. These three variables are: the peripheral velocity vector of the blade element (ωr), the absolute velocity vector (V), and the relative velocity vector (V_R). Figure 5 shows how these vectors are influenced when progressing through the turbine stage.

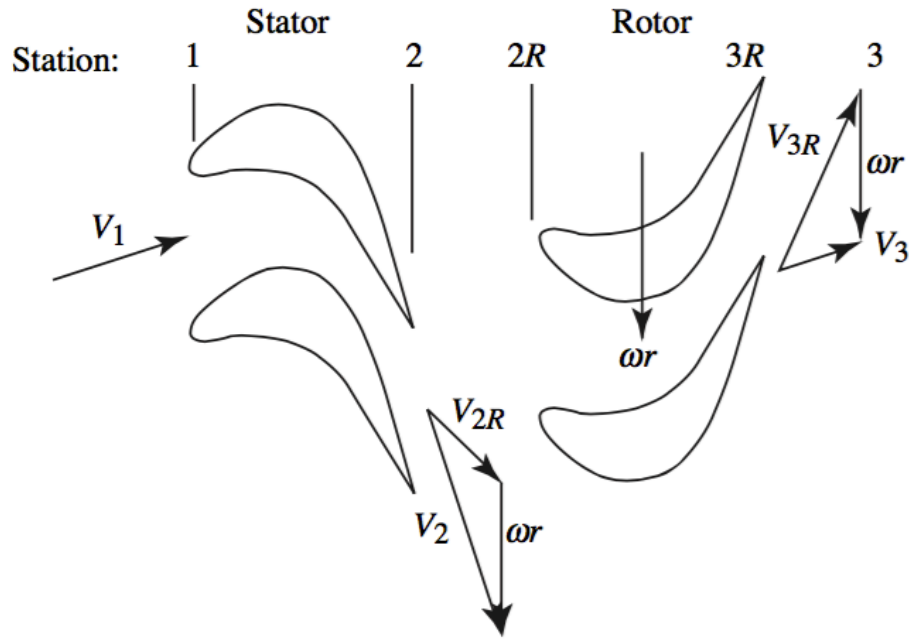


Figure 5: Velocity Vectors for Stator and Turbine (Mattingly, 2000)

The use of velocity triangles and diagrams is crucial to turbine and stator design. Thrust for example, is influenced by the velocity vector that points in the axial direction of the turbine. Sometimes called the thrust vector, this velocity can be determined using the following equation.

$$V_3 = \omega r \tan(\beta_3)$$

Equation 4: Thrust Vector (Shreckling, 1992)

where,

V_3 = Absolute speed of exhaust gas

ωr = Peripheral speed of turbine blade

β_3 = Angle between V_{3r} and ωr (relative speed of exhaust gas)

Turbine rotors encounter extremely high temperatures and rotational speeds which result in high centrifugal forces and therefore high stress in the blades. The centrifugal force on a turbine blade can be calculated using Equation 5:

$$F = \rho A \omega^2 \left(\frac{r_1^2 - r_2^2}{2} \right)$$

Equation 5: Centrifugal Force Calculation (npower, 2009)

where,

$\rho = \text{Density of the turbine blade material} \left(\frac{kg}{m^3} \right)$

$A = \text{Cross sectional area of the blade} (m^2)$

$\omega = \text{Angular velocity} \left(\frac{radians}{second} \right)$

$r_1 = \text{Rotor disk radius} (m)$

$r_2 = \text{Blade tip radius} (m)$

From here, it is possible to calculate the nominal stress on the blade root with Equation 6:

$$\sigma = \frac{F}{A_{root}}$$

Equation 6: Blade Root Nominal Stress

Where A_{root} is the cross-sectional area of the blade root, which in in this project is equivalent to the cross-sectional area of the blade, A , due to a constant cross-sectional blade design. This nominal stress should be accounted for when selecting blade material to ensure that the blades can withstand the centrifugal force. Turbine rotors often require high safety factors, making sure that this nominal stress is magnitudes lower than the

allowable tensile strength of the material used. It should be noted that the center of the turbine wheel experiences centrifugal forces up to three times as high as the blades due to a stress concentration at the hole (Kamps, 2005). Common turbine wheel designs account for this by employing a thicker center of the disk than along the outsides.

2.2.D. Combustion Chamber

The purpose of the combustion chamber is to retrieve air from the compressor stage and deliver it at much greater temperatures to the turbine stage, this is where heat is added to the cycle by burning fuel. The diffuser section of the compressor stage decelerates the airflow in order to increase pressure before it reaches the combustion chamber. This high-pressure air stores potential (pressure) energy and will produce better combustion and cycle efficiency. Energy is further increased through combustion of injected fuel, usually kerosene, and the high-pressure air (Hunecke, 1997). Average air/fuel ratios range from around 45:1 to 130:1 for the entire combustion chamber however fuel will only burn efficiently around the stoichiometric air/fuel ratio, 15:1. As this project is concerned with combustion chamber design, it should be noted that many advancements in combustion chamber design have been founded upon empirical data and experimentation (NASA, 1973). Therefore, design of combustion chambers relies heavily on the analysis of previous, similarly designed systems.

Two common types of combustion chambers have been developed, the cylindrical, or can chamber, and the annular chamber. A single annular chamber can be employed quite effectively in a turbojet engine while being conducive to minimizing weight, cost,

and complexity of design (Smith, 1956). Our research focuses on small, annular combustion chambers that can be utilized in miniature turbojet engines.

Similar to the turbine stage, the combustion chamber must account for extremely high temperatures. For this reason, nickel-based super alloys are often used for this component. Conditions that constitute an effective combustion stage design include: continuous combustion, uniform combustion (no hot spots), adequate mixing of air and fuel, low pressure losses, and short length to cross-sectional area ratio. Figure 6 shows an example of an annular combustion chamber.

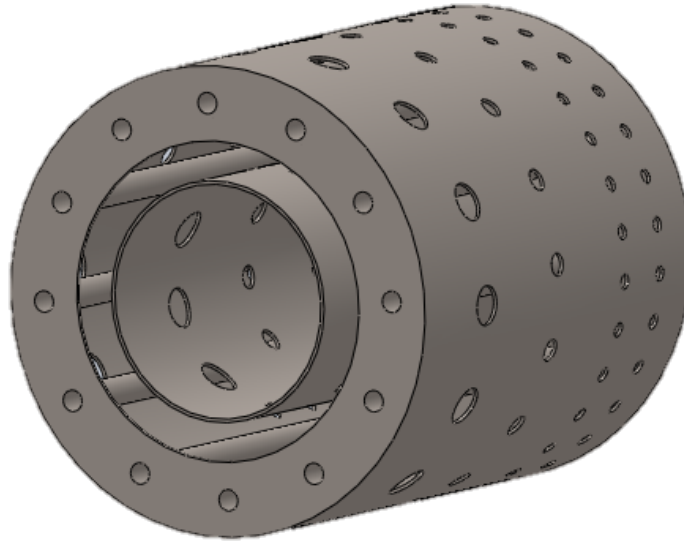


Figure 6: Example of an Annular Combustion Chamber

The combustion chamber is broken down into three zones: the primary, secondary, and tertiary zones (Smith, 1956). These three different zones can be associated with the three distinct hole sizes on both the outer and inner liner of the combustion chamber. The largest holes make up the primary zone, the second largest make up the secondary zone, and the smallest holes make up the tertiary zone. Often,

these holes are plunged in order to act as small nozzles and accelerate the incoming air. The gas mixture ignites, traditionally through the use of a spark plug, in the primary zone which is the first combustion zone downstream the compressor. The secondary zone is where further air is injected and the combustion process is completed. The last section, the tertiary zone, is where any leftover air is injected to achieve air temperatures sufficient for entry into the turbine stage.

In order for a combustion chamber to be effective, continuous combustion must be achieved so that the heat from a previous reaction is sufficient to vaporize the liquid fuel for the next reaction. High initial temperatures, high fuel to air ratios and high pressures are necessary for this continuous combustion (El-Sayed, 2015). If the fuel to air ratio is too low, then heat generated from the reaction is mostly spent in increasing the temperature of nitrogen and oxygen in the chamber rather than vaporizing the incoming fuel. In order to achieve this self-sustaining combustion, engines are often started with an alternative gaseous fuel source, such as propane. This allows for the engine to achieve sufficient temperatures before introducing kerosene and risking partial combustion that could result in carbon build up that can gunk up the engine or cause hot spots.

2.2.E. Exhaust Nozzle

The purpose of an exhaust nozzle is to create thrust by converting the potential energy of incoming gas into kinetic energy (Hunecke, 1997). In the nozzle, the mass flow rate is constant. As velocity increases in the direction of flow, pressure decreases. Typically, length is not a crucial design consideration however, losses due to friction can be excessive if the nozzle is too long. In an ideal nozzle,

there are minimal kinetic energy losses due to this friction. Well-designed nozzles can commonly achieve efficiencies up to 90%.

Common nozzle designs for aircraft include the converging nozzle and the converging-diverging nozzle. Converging nozzles are used for aircraft flying at subsonic speeds, speeds which are less than the speed of sound throughout the nozzle. Converging-diverging nozzles are used to achieve supersonic flows, which are typically used in military aircraft. Flow through convergent nozzles are subsonic when the pressure at the exit is equal to ambient pressure (Hill & Peterson, 1992). The exit area of a convergent nozzle is known as the throat. This project focuses on the use of a converging nozzle in order to reduce noise and avoid shockwaves.

Theoretical converging nozzle analysis uses some basic assumptions: frictional losses between the air and the walls are neglected, the gases are treated as ideal gases, the process is steady state and steady flow, the process is isentropic, and mass and energy are conserved through the nozzle (Smith, 1956). These assumptions aid in the design of nozzles, however small jet engines have been successful using a very simple converging nozzle design with minimal reduction in cross sectional area across the nozzle. This is done in order to avoid choked flow at the exit (Benini & Giacometti, 2007).

2.2.F. Fuel System, Lubrication & Bearings

Gas turbines can utilize an assortment of liquid or gaseous fuels. Gaseous fuels do not require vaporization to achieve combustion. However, liquid fuels present a lower risk of gas escape and are therefore easier to handle and store. For this reason, liquid fuels are common in aircraft engines. The desirable characteristic when choosing a fuel source is a high specific heat of combustion. Also known as the specific energy, this property is defined as the energy per unit mass of a fuel (Shreckling, 1992). High specific energy results in lower quantities of fuel needed to achieve high levels of energy production. Common turbine fuels include: diesel, kerosene, propane and butane, which all have specific energy values ranging from 40-50 MJ/kg. Table 1 shows some common specific energy values for different fuel sources.

Table 1: Specific Energy and Density of Different Fuels

Fuel	Specific Energy (MJ/kg)	Density (kg/m³)
Methane	55.6	423
Propane	50.3	585
Butane	49.5	601
Gasoline	47.3	716
Kerosene	46.2	830
Diesel	44.8	830

The stoichiometric air/fuel ratio of the mixture is essential to achieving combustion. This ratio defines the amount of air consumed by the engine compared to the amount of fuel consumed. For example, gasoline engines require an air/fuel ratio of 14.7:1, meaning for every 1 part of fuel, 14.7 parts of air are required to achieve combustion. The proper mixture of fuel and air is critical in achieving high engine durability and performance. Any excess fuel will not combust and form deposits on combustion chamber components such as injectors, vaporization tubes or even turbine blades (Flack, 2005). This can further lead to the development of hotspots and inefficient combustion. Another important consideration is determining the minimum required fuel consumption for the engine. By calculating the heat output and then using the specific density and energy of the fuel, the minimum fuel flow requirement can be determined.

$$\dot{Q} = \dot{m}c\Delta T$$

Equation 7: Thermal Output Equation (Shreckling, 1992)

Where,

$\dot{Q} = \text{Heat output (W)}$

$c = \text{Specific heat of air } \left(\frac{\text{KJ}}{\text{kgK}} \right)$

$\dot{m} = \text{Mass flow rate}$

$\Delta T = \text{Change in temperature across engine}$

$$F = \frac{\dot{Q}}{e\rho}$$

Equation 8: Fuel Flow Required (Shreckling, 1992)

where,

$$F = \text{Minimum fuel flow} \left(\frac{\text{mL}}{\text{s}} \right)$$

$$e = \text{Specific Energy of fuel} \left(\frac{\text{KJ}}{\text{kg}} \right)$$

$$\rho = \text{Density of fuel} \left(\frac{\text{kg}}{\text{mL}} \right)$$

In order to burn liquid fuels effectively, the fuel must first be vaporized and then be mixed with oxygen. One method of vaporizing liquid fuel is the integration of vaporization tubes inside the combustion chamber. These tubes act as heat exchangers between the cold liquid fuel and surrounding hot gases. The temperature of the combustion chamber must be high enough so that vaporization can occur using liquid fuels (Shreckling, 1992). To achieve these temperatures, gaseous fuels can be used as a method to starting small gas turbine engines in order to attain full vaporization.

2.3 Ideal Cycle Analysis

The goal of cycle analysis with regard to design of gas turbines is to develop values for performance parameters. Thrust, fuel consumption, and other important values can be calculated based on a number of assumptions and design specifications (Oates, 1997). These assumptions and specifications are as follows:

Assumptions

- Compression and expansion are isentropic and adiabatic processes
- The working fluid is taken as an ideal gas with constant specific heat specific heat ratio
- Heat for combustion is assumed to come from an outside source and the fuel mass is neglected

Specifications

- Compression ratio indicated prior to design
- Ambient air temperature and pressure are known
- An inlet Mach number is indicated

2.3.A. The Brayton Cycle

Jet engines operate as an open Brayton Cycle where a working fluid flows into a compressor, is combusted, and then exhausted through a turbine (El-Sayed, 2015). Unlike a closed system, these exhaust gases cannot be recirculated as they are instead used to generate thrust. Figure 7 represents a typical open Brayton Cycle where a negligible mass of fuel is injected at the combustor stage.

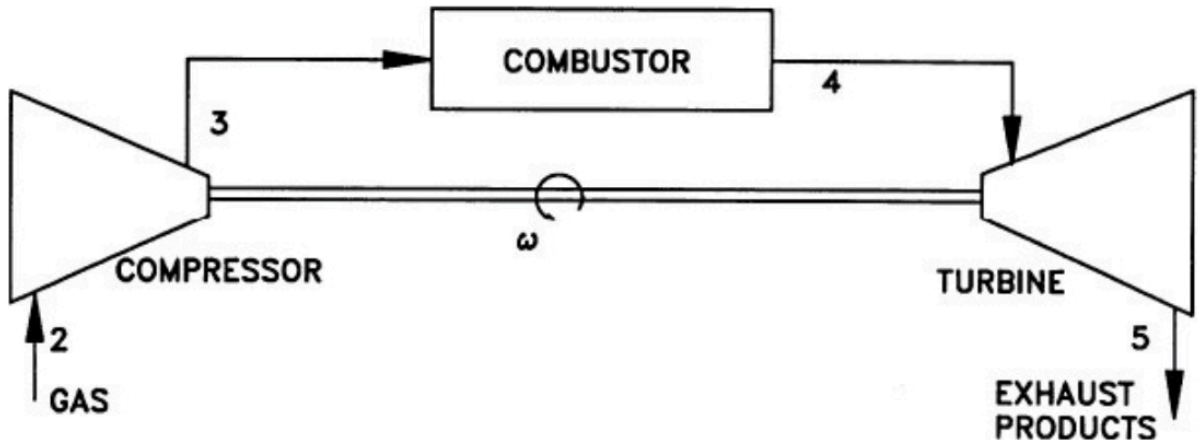


Figure 7: Example Geometry of Open Brayton Cycle (Flack, 2005)

The compressor and turbine are connected by a single shaft with an angular velocity. When considering an aircraft gas turbine, the work of the engine can be viewed as the change in kinetic energy between the incoming and outgoing fluid (Oates, 1997). The stages of a gas turbine related to the location on the engine can be defined as follows:

Table 2: Stages of Gas Turbine Engine

Stage	Location
0	Upstream
1	Inlet Entry
2	Compressor Entry
3	Compressor Exit
4	Turbine Entry
5	Turbine Exit
6	Nozzle Entry
7	Nozzle Exit

Figure 8 represent the Brayton Cycle. These temperature-specific volume, pressure-specific volume, and temperature-entropy diagrams are commonly used to observe the changes in these properties between different stages of the engine.

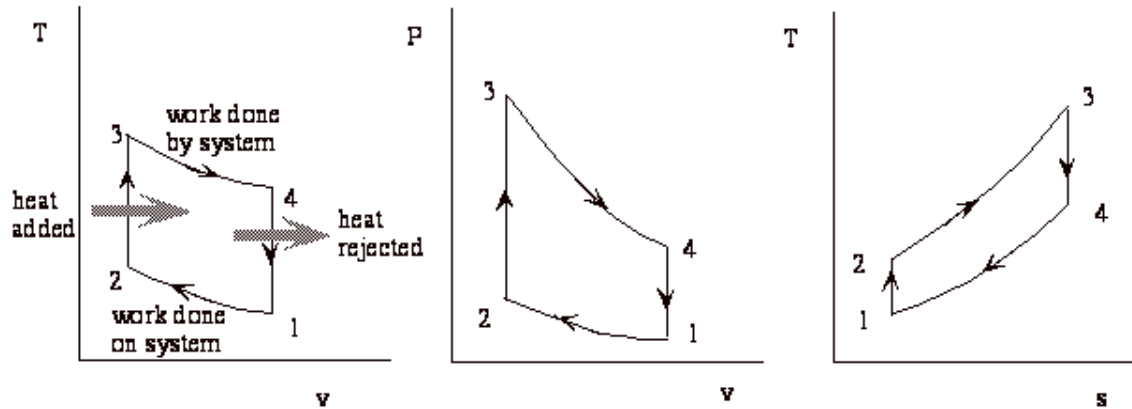


Figure 8: T-v, P-v and T-s Diagrams (MIT, 2014)

The four processes that constitute the Brayton Cycle can be seen in these diagrams. These processes are:

- $0 \Rightarrow 3$ Isentropic Compression
- $3 \Rightarrow 4$ Constant Pressure Combustion
- $4 \Rightarrow 8$ Isentropic Expansion
- $8 \Rightarrow 0$ Constant Pressure Heat Rejection
(Fluid is not recirculated in open cycle)

The following section introduces the equations related to each component when observed using the ideal cycle analysis.

2.3.B. Ideal Component Analysis

By determining the pressure and temperature at the first stage of the cycle, pressures and temperature downstream can be calculated. To achieve this, these properties are taken as ratios across each component. The ideal analysis for our engine follows the following equations and can be seen in Appendix A.

$$\text{Pressure Ratio } (\pi) = \frac{\text{Stagnation Pressre Leaving Component}}{\text{Stagnation Pressure Entering Component}}$$

$$\text{Temperature Ratio } (\tau) = \frac{\text{Stagnation Temperature Leaving Component}}{\text{Stagnation Temperature Entering Component}}$$

Inlet

Flow across the inlet is assumed to be isentropic and adiabatic. Throughout the inlet, there is no change in pressure or temperature and the enthalpy is constant. Therefore,

$$\pi_i = \frac{\text{Pressure at Compressor Entry}}{\text{Free Stream Air Pressure}} = \frac{P_2}{P_0}$$

Equation 9: Pressure Ratio Across Inlet

$$\tau_i = \frac{\text{Temperature Compressor Entry}}{\text{Free Stream Air Temperature}} = \frac{T_2}{T_0}$$

Equation 10: Temperature Ratio Across Inlet

Compressor

The compressor has pressure and temperature ratios that are not constant.

Enthalpy, temperature and pressure increase across the compressor as energy is added to the fluid.

$$\pi_c = \frac{\text{Pressure at Compressor Exit}}{\text{Pressure at Compressor Entry}} = \frac{P_3}{P_2}$$

Equation 11: Pressure Ratio Across Compressor

$$\tau_c = \frac{\text{Temperature at Compressor Exit}}{\text{Temperature at Compressor Entry}} = \frac{T_3}{T_2}$$

Equation 12: Temperature Ratio Across Compressor

Because flow is considered isentropic across the compressor, the two ratios can be related using the following equation:

$$\pi_c = \tau_c^{\frac{\gamma}{\gamma-1}}$$

Equation 13: Compressor T-P Relation (NASA, Compressor Thermodynamics, 2015b)

where,

$\gamma = \text{Specific heat ratio}$

If the pressure ratio across the compressor is specified and the inlet temperature and pressure are known, the conditions at the exit of the compressor can be found.

Furthermore, the compressor work can be calculated using the relation:

$$W_c = c_p(T_3 - T_2)$$

Equation 14: Compressor Work (NASA, Compressor Thermodynamics, 2015b)

where,

$$c_p = \text{Specific heat of air} \left(\frac{\text{KJ}}{\text{kgK}} \right)$$

Combustor

During combustion pressure remains constant and temperature increases, resulting in:

$$\pi_b = \frac{\text{Pressure at Turbine Entry}}{\text{Pressure at Combustor Exit}} = \frac{P_4}{P_3}$$

Equation 15: Pressure Ratio Across Combustor

However, temperature does increase and is calculated using:

$$\tau_c = \frac{\text{Temperature at Turbine Entry}}{\text{Temperature at Compressor Exit}} = \frac{T_4}{T_3}$$

Equation 16: Pressure Ratio Across Combustor

The heat input and the minimal fuel requirements for combustion can be found using Equations 7 and 8 shown in Chapter 2.1.E.

Turbine

Temperature and pressure both drop across the turbine stage due to the fact that energy is being removed from the fluid in order to rotate the shaft.

$$\pi_t = \frac{\text{Pressure at Turbine Exit}}{\text{Pressure at Turbine Entry}} = \frac{P_5}{P_4}$$

Equation 17: Pressure Ratio Across Turbine

$$\tau_t = \frac{\text{Temperature at Turbine Exit}}{\text{Temperature at Turbine Entry}} = \frac{T_5}{T_4}$$

Equation 18: Temperature Ratio Across Turbine

Because flow is also considered isentropic across the turbine, the two ratios can be related using the following equation:

$$\pi_t = \tau_t^{\frac{\gamma}{\gamma-1}}$$

Equation 19: Turbine T-P Relation (NASA, Turbine Thermodynamics, 2015d)

Furthermore, turbine work can be calculated using the relation:

$$W_t = c_p(T_5 - T_4)$$

Equation 20: Turbine Work (NASA, Turbine Thermodynamics, 2015d)

Nozzle

Flow across the nozzle is also to be assumed isentropic and adiabatic.

$$\pi_n = \frac{\text{Pressure at Nozzle Exit}}{\text{Pressure at Nozzle Entrance}} = \frac{P_8}{P_7}$$

Equation 21: Pressure Ratio Across Nozzle

$$\tau_n = \frac{\text{Temperature at Nozzle Exit}}{\text{Temperature at Nozzle Entrance}} = \frac{T_8}{T_7}$$

Equation 22: Temperature Ratio Across Nozzle

3.0 Methodology

This chapter explains how we designed and manufactured each component of our engine. We present each component and outline the considerations and challenges encountered during the design process. Additionally, we discuss the materials and manufacturing methods used to produce each component. We have included the two-dimensional CAD drawings of each part in Appendix D.

3.1 Compressor

In order to simplify the design and manufacturing process and complete the project within the given time constraint, our team decided to purchase a compressor wheel. After examining the literature regarding compressor wheels used in small gas turbine engines, we concluded that a single stage axial compressor would not offer a high enough compression ratio or efficiency to be used in an engine of our size. Engines similar in size to our own design, such as the SR-30 described in Chapter 2.2, utilize a centrifugal compressor in order to achieve adequate compression ratios and efficiencies. For these reasons, we chose to investigate centrifugal compressor wheels used in automotive turbochargers. We found that the Garret GT4202 compressor wheel provided a mass flow rate and pressure ratio, at our desired RPM, similar to those recorded in SR30 test data (Witkowski, White, Ortiz Duenas, Strykowski, & Simon, 2003). Additional benefits of selecting this compressor were its availability for purchasing and the accessibility of its compressor map. The compressor map for the GT4202 can be seen in Figure 9.

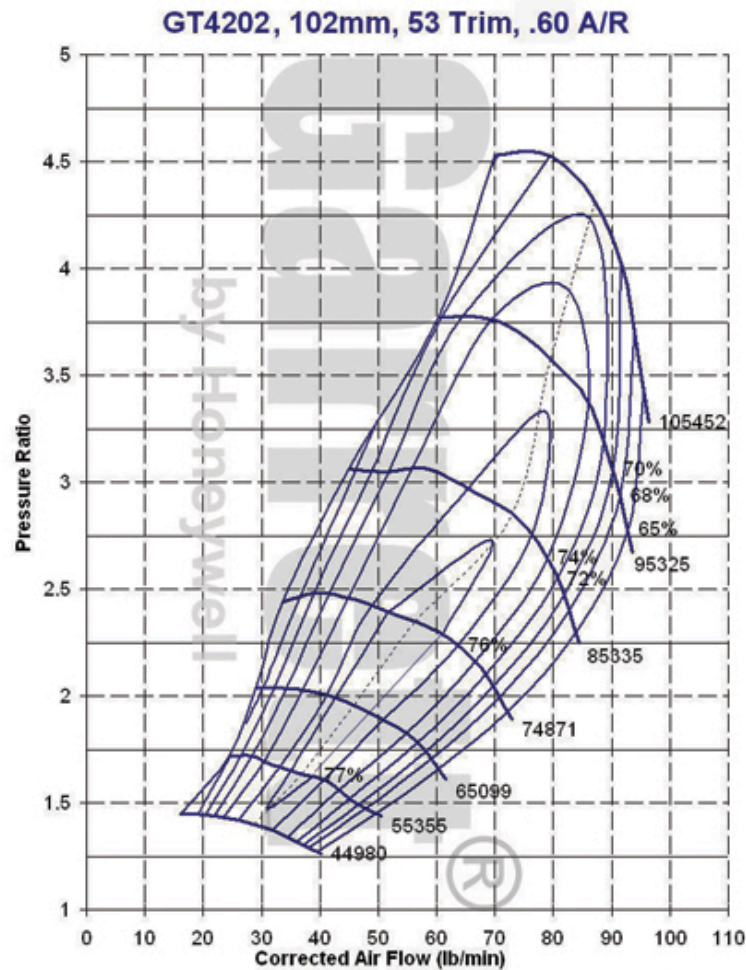


Figure 9: GT4202 Compressor Map (Limit Engineering, 2015)

The GT4202 incorporates a curved profile on the diffuser side. We quickly realized that removing the profile and machining the diffuser side flat would allow us to more easily match this compressor to a diffuser without the need to match this unknown profile. Therefore, we decided to machine the diffuser side flat using a manual mill. Pictures of the altered GT4202 compressor attached to the shaft can be seen in Figure 10.



Figure 10: G4202 Attached to Drive Shaft

3.2 Inlet Shroud

The primary challenge we faced while integrating the GT402 compressor into our engine design was obtaining the profile of the rotating compressor wheel. Computer Aided Design (CAD) models of the compressor are proprietary and unavailable to consumers. However, it was essential that we find these dimensions in order to design an inlet shroud. The space between the compressor blades and the inlet shroud cannot exceed $40/1000$ of an inch and to achieve reasonable efficiencies, should be as small as possible (Kamps, 2005). Therefore, our team was forced to find a way of designing a shroud to meet this high tolerance.

After considering the use of a Coordinate Measuring Machine (CMM) as well as an Optical Comparator, we determined the best course of action was to obtain a 3D scan of the compressor. We reached out to a company in Windsor, Connecticut called Capture 3D, their staff donated their time, equipment, and expertise to generate a stereolithographic (STL) file of our compressor wheel. We then imported this STL file into SolidWorks. In order to design the inlet shroud to match the curvature of the rotating compressor profile, we drew concentric circles around the fins of the compressor and connected them with a spline. Rotating this spline around a centerline generated a surface matching the compressor profile. By offsetting this surface, we were able to design an inlet shroud that is within the acceptable tolerance.

The shroud was machined from a six-inch bar stock of 6061 t651 aluminum and was turned on a Computer Numerical Control (CNC) lathe in the Worcester Polytechnic Institute (WPI) Washburn Shops. A total of sixteen bolt holes were drilled around the perimeter of the shroud in order to facilitate assembly. The completed inlet shroud can be seen below in Figure 11.

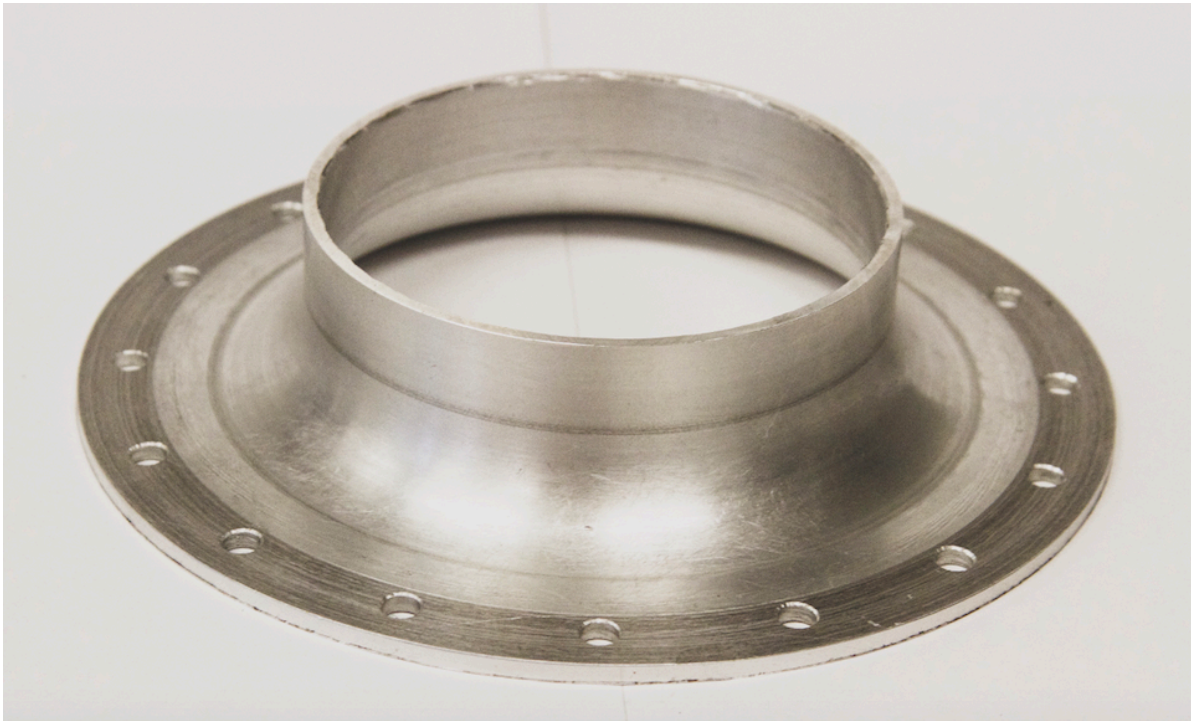


Figure 11: Inlet Shroud

3.3 Diffuser

The first decision to be made when designing the diffuser stage was which diffuser style to choose: veined or channel. After reviewing the literature on small gas turbine engines and other similar designs, we chose the wedged channel diffuser design. This same style diffuser was used successfully in the KJ66 engine. Additionally, the wedges provide a convenient location to drill bolt holes in order to fasten the inlet shroud. Considering the diffuser does not experience extremely high temperatures, we decided to machine it from 6061 t651 Aluminum. Aluminum provided us with adequate strength for the components purpose, while enabling an easier machining process.

We machined the part on a Haas VM-2 vertical milling machine. After the operation to machine the wedges was completed, we drilled the holes with a separate CNC program and hand tapped the holes. In order to machine the vanes on the side of the diffuser, we fixed the stock in an indexing head and moved the indexing head a determined angle evenly properly locate the fins. Finally, we implemented a program to machine the holes on certain fins. The completed diffuser can be seen in Figure 12.

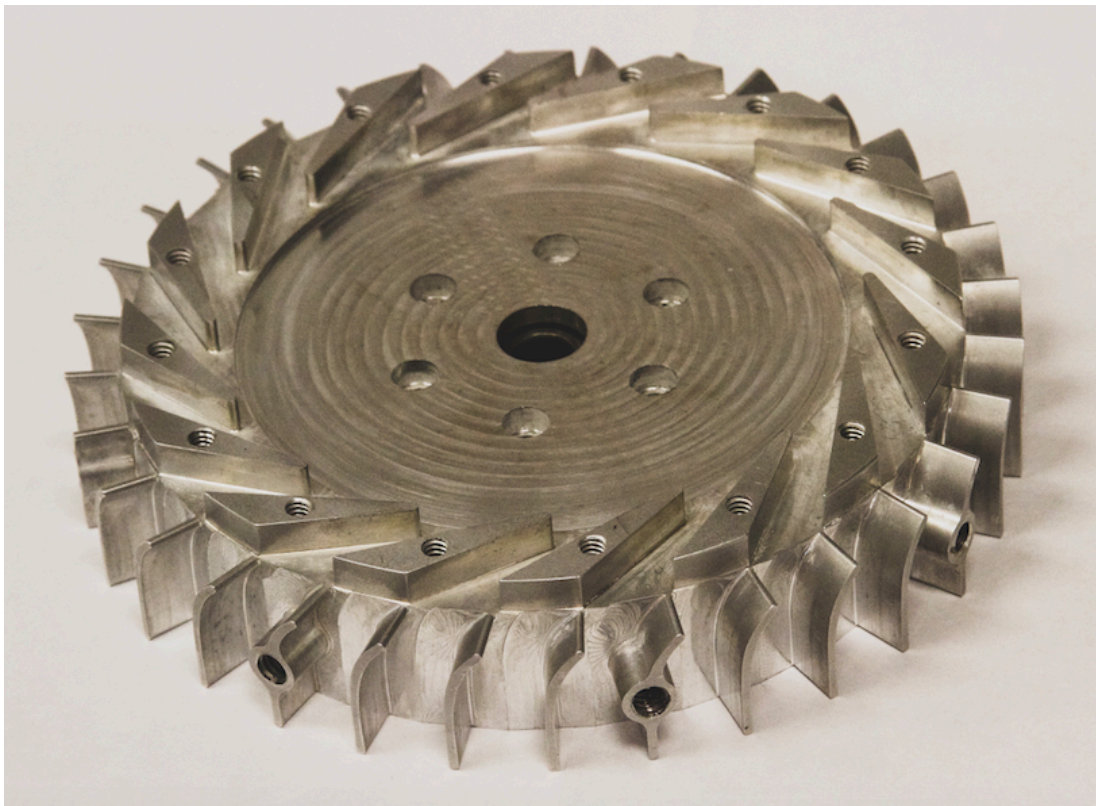


Figure 12: Channel Diffuser

3.4 Combustion Chamber

Based on the literature reviewed, our team decided to manufacture an annular combustion chamber. Annular combustion chambers allow the manufacturer to create an engine of smaller diameter, which we found to be desirable. Additionally, we determined utilizing another combustion chamber design, such as the can combustor, would have provided a more substantial manufacturing challenge. Because most combustor design is based off empirical data, and we were not focused on optimizing a design, we decided to model our combustor after successful combustion chambers that have been widely implemented on turbocharger based amateur gas turbine engines.

Our combustion chamber design incorporates an outer line and inner flame tube. Both of which contain 3 separate zones of holes. Primary, secondary, and tertiary holes in the combustor that assist the mixing of air and fuel. Due to its ability with withstand extremely high temperatures, we chose to manufacture our combustion chamber out of Inconel 625. A local company donated a 0.02-inch-thick sheet of the material which we then cut into four pieces. We rolled two pieces into the inner flame tube and outer line while the remaining two pieces were cut into two annular end caps. We then welded eight vaporization tubes, about 5 inches long and $\frac{1}{4}$ inch diameter, to the turbine side endcap. Finally, the two caps were welded to the outer line and the compressor side cap was welded to the flame tube, completing the assembly. An image of the completed combustion chamber can be seen in Figure 13.



Figure 13: Combustion Chamber

3.5 Shaft Housing

We designed the shaft housing to accommodate the shaft and bearing dimensions. There is substantial flexibility regarding the design of the housing outer profile, various models can be seen throughout the world of miniature gas turbines. We decided to go with a simple, straight profile that widens at one end to allow space for bolt holes to fix the housing to the diffuser. The inner tube incorporates two bearing seats. The bearing seat at the diffuser end, which can be seen in Figure 14, accommodates half of the bearing thickness. When bolted to the diffuser, the shaft housing sandwiches the bearing halfway between the diffuser and

the housing. The turbine end bearing seat is designed to allow space for a spring and sleeve system which places ten pounds of preload on the bearing. The purpose of this system is to increase the longevity of the bearing when experiencing high rotational speeds and temperatures near the turbine.

The shaft housing was manufactured from a three-inch diameter, 6061 t651 aluminum rod. We first drilled and then bored the inside diameter to accompany the shafts dimensions. We then drilled and bored the inner area on the turbine side to accommodate the sleeve spring system and turned down the outside. The component was then flipped, centered and then bored and turned again to achieve the features on the compressor side. Finally, eight holes were drilled on the base on the shaft housing in order to fixture it to the diffuser. The completed shaft housing can be seen in Figure 14.



Figure 14: Shaft Housing

3.6 Fuel Distributer

The purpose of the fuel distributor is to transport fuel from an outside source into the vaporization tubes of the combustion chamber. We chose a simple distributor designed similar to those seen in many small gas turbines. The distributor consists of eight, 0.08-inch diameter fuel injectors mounted normal to our $\frac{1}{4}$ inch injector ring. Each injector is matched to a corresponding vaporization tube on the turbine side endcap of the combustion chamber. The injector ring sits on the outside of this endcap where it is held in place by the stator housing. Tubing connects to the ring which runs alongside the length of the combustion chamber and through the outer case of the engine. It is here where the distributor connects to an outside fuel source.

The fuel distributor was manufactured entirely from 316 stainless steel tubing. We first cut and rolled the larger tubing to make the five-inch diameter injector ring. Next, we drilled eight 0.08-inch diameter holes in the injector ring to accommodate the fuel injectors. An additional hole was drilled perpendicular to these holes for the fuel supply line. We then cut eight, 0.08-inch diameter fuel injectors each 3 inches in length. We determined that conventional welding methods would not be feasible due to the small diameter and wall thickness of the tubing. Therefore, we decided to reach out to a local company with laser welding capabilities. They agreed to weld the assembly together and the resulting fuel distributor can be seen in Figure 15.

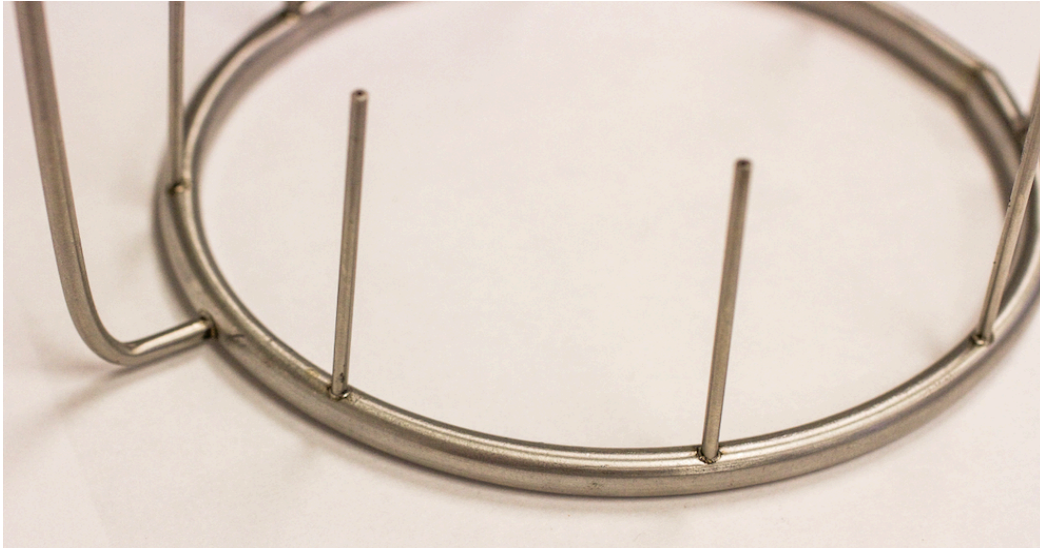


Figure 15: Fuel Distributor

3.7 Turbine

The development of airfoils and turbines for new engines is a subject of years of study and it was impossible to design and test our own original airfoils.

Therefore, to simplify turbine design we chose the NACA 23012, a common airfoil used for turbine blades. In order to ensure that the turbine rotor could handle the centrifugal forces experienced at high angular velocities, the stress at the roots of the blade were calculated and compared to the allowable tensile strength of the material. These stress calculations can be found in appendix B.

The turbine was initially designed to be machined from Inconel 718 four-inch bar stock due to the material's ability to maintain strength during high temperature rotation. In order to achieve the desired airfoil geometry and a curved channel floor between fins, we attempted to complete the machining operation in a mill with 5-axis capability. However, our first attempts at machining the Inconel proved quite

difficult. Machining the channels between our fins required a 1/8" end mill. From speaking with WPI shop staff and consulting popular online machinist forums, we found that it is nearly impossible to avoid breaking 1/8" carbide end mills while machining Inconel for an extended period. We considered a variety of feeds and speeds, lubrication techniques, and tool paths in order to design a more efficient machining procedure for the turbine fins. However, we eventually determined that machining our turbine from Inconel 718 would incur too great of a financial cost and consume more than an acceptable amount of our time table.

The failure of the Inconel turbine consumed an excessive amount of our time. Our initial attempts to machine the turbine from the Nickel super-alloy resulted in multiple broken end mills per blade and the machining operation was calculated to take upwards of twenty hours. In retrospect, we became too attached to the idea of using Inconel and committed to troubleshooting the problem instead of making an early decision to change the material. Eventually, we decided to machine the turbine from a disk of 316 stainless steel thus greatly reducing the machining time, tooling cost, and difficulty.

The primary change in design, apart from the material, was a transition from a curved channel floor to a flat channel floor. The ramifications of this change are likely to be a slight decrease in efficiency due to the sharper edge of the blade channels. Additionally, 316 stainless steel does not maintain strength at elevated temperature as well as Inconel. Therefore, the change also decreased the turbines critical rotational speed. On the positive end, this decision decreased our machine

time, machining cost, and labor. However, after we completed the turbine and attached it to our shaft, we realized that the turbine was slightly asymmetrical.

We determined the most likely cause of asymmetry in the turbine to be a failure in properly fixturing the component during CNC operations, resulting in the stock piece being not perfectly centered in the lathe chuck. As a result, the turbine blades on one side of the disk were machined approximately 20/1000 in shorter than those on the other side. Due to the difference in the length of the blades, we were forced to either re-machine the rotor or remove 20/1000 in from the overall diameter. We determined that we did not have enough time to machine a second turbine and decided to repair the original. The resulting turbine, prior to balancing, produced substantially less vibration when spun with compressed. However, the alterations to the blade length resulted in a gap between the turbine and the stator housing of 30/1000 in. The specified tolerance between these two parts was 10/1000 in in order to achieve minimal gap losses and maximize efficiency. Although the turbine will be adequate for operation it is not ideal and will suffer from unnecessary gap loss during operation. The completed turbine wheel attached to the shaft can be seen in Figure 16.



Figure 16: Axial Turbine

3.8 Outer Casing & Inlet Flange

Perhaps the simplest component to design was the outer casing. A six-inch diameter tube with eight bolt holes placed around the circumference of the compressor side. Bolts passing through these holes secure the inlet flange, outer casing and diffuser into a rigid body and ensure that the spacing between compressor and shroud is maintained. While the compressor end is enclosed by the compressor and inlet shroud assembly, the turbine end is enclosed by the stator housing and an annular endcap.

We chose to manufacture the outer housing from a six-inch outer diameter length of 304 stainless steel tubing. The primary challenge during manufacturing was properly holding the tube on a lathe in order to machine the outer and inner diameters. Due to the size and length of the tube, we decided to use a four-jaw chuck to hold it from the inside. We encountered a large amount of deflection and chatter while turning down the outer diameter. To solve this problem, we welded a piece of steel across the inside diameter of one end of the tubing. We then center drilled the piece of steel and utilized a tailstock and live center to reduce deflection and ensure a uniform surface finish. Following the turning operation on the outer diameter, we flipped the tube and bored the inside to the exact outer radius of the diffuser fins. Once the tube diameters were properly sized, we drilled eight holes around the circumference of the diffuser end and welded an annular endcap to the turbine side. The primary feature of the annular endcap is to allow for the attachment of the nozzle. The outer housing can be seen in Figure 17.

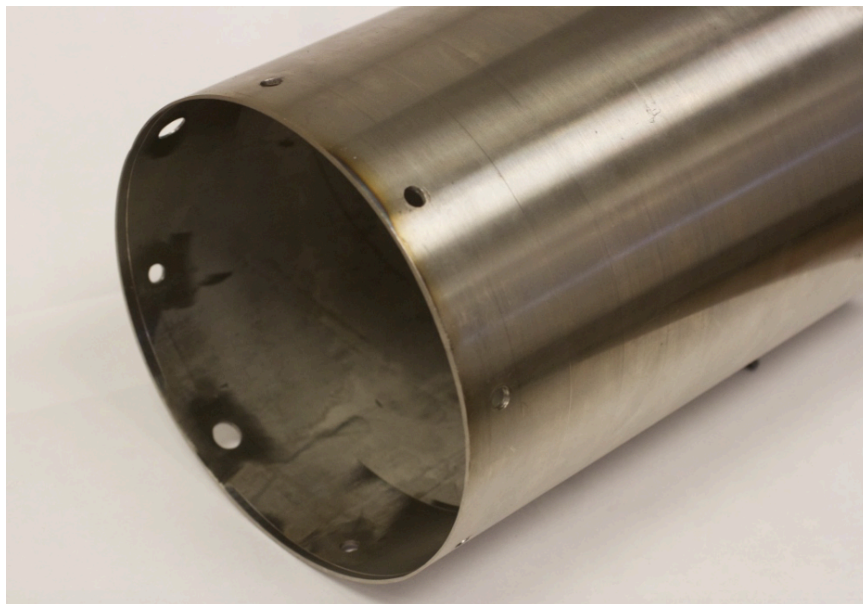


Figure 17: Outer Casing

We also designed and manufactured a simple inlet flange to cover the compressor side of the outer casing and hold the assembly, and engine, together. We designed the flange to fit loosely over the outer casing to allow proper spacing for gasket material. Bolt holes placed around the perimeter of the flange line up with holes on the casing and diffuser. We machined the flange from 7-in diameter 6061 t651 aluminum stock. The machining operation was performed on a HAAS VM-2 utilizing Esprit. We used ½-in end mills to pocket the material and a 3-in face mill in order to give it a flat surface finish. We also drilled the holes on the side using an indexing head and the manual mill. The completed flange can be seen in figure 18.

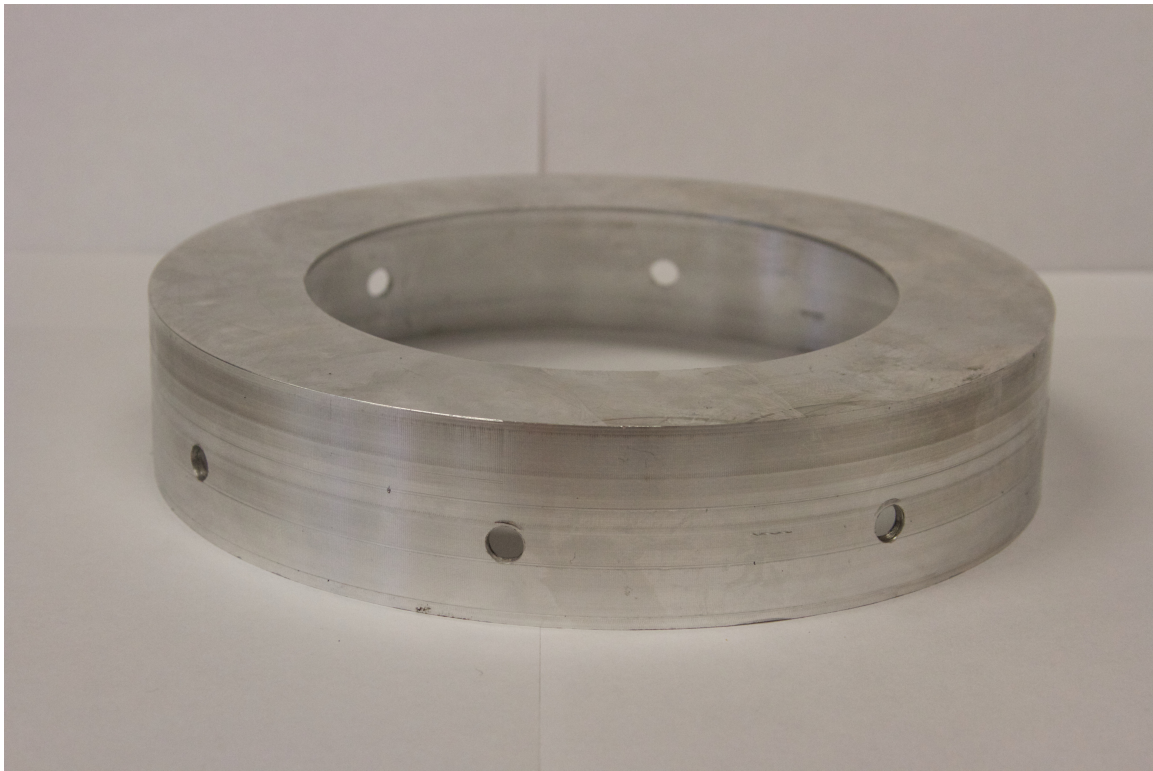


Figure 18: Inlet Flange

Minimizing gap losses and ensuring a tightly sealed engine is crucial to the efficiency of gas turbines. In addition to the turbine, the seal between the outer casing and the flange is an area of concern for gap losses in our engine. Because the flange is bolted to the housing, it is necessary to implement a gasket between the two parts in order to eliminate any leaks. We initially decided to use gasket paper between the two parts but once the engine was assembled we found that the gasket paper did not provide a reliable seal. We decided that a simpler method might be to seal the gap with a high temperature silicon gasket sealer. The silicon sealer can better fill any small gaps or leaks that might be formed in gasket paper when securing the flange.

3.9 Shaft

After reviewing various shaft designs used in similar engines, such as the KJ66 and SR30, we decided to use a design very similar to the KJ 66. Our engine is slightly larger than the KJ 66 therefore, we scaled up the shaft design while maintaining the overall style.

The shaft, made of 316 stainless steel, was cut to about 11.5-in in length and then turned down on a lathe to meet our specifications. The design includes a taper on each side of the shaft intended to decrease stress concentrations and eliminate the sharp edges that might infringe upon lubricant flow through the shaft housing. There are two locator steps/bearing seats that serve to position the bearings on each end, these steps are machined to allow a light press fit upon bearing installation. In order to ensure that the shaft was manufactured to be concentric

and as balanced as possible, we utilized an indicator to establish a true rotation in the chuck whenever the workpiece needed to be manipulated. Additionally, during any turning operations the shaft was held by a live center tailstock to minimize the chances of deflection and inaccuracies. To complete the shaft, we cut left hand threads into each end in order to accommodate the turbine and compressor. The shaft can be seen in Figure 19.



Figure 19: Shaft Assembly

3.10 Stator & Stator Housing

The stator housing was designed to be machined from 316 stainless steel bar stock. The primary purpose of the housing is to hold the stator in place and allow the turbine to rotate at full speed while maintaining the high tolerance necessary for efficiency. We designed a simple geometry which includes a simple thin walled hollow cylinder with a flange on either end. The flanges provide surfaces where the combustion chamber and exhaust nozzle can be attached. On the combustion side, the flange was designed to be welded to the combustion chamber while the nozzle could be attached with bolts feeding through small tabs on the nozzle and into the housing.

The stator was machined in the same fashion as the turbine. Once, we machined the stator as a bladed disk, we then installed the disk into the stator housing and welded the blades to the outer walls. The stator housing was machined using 35° and 55° ferrous inserts and a ferrous boring bar to bore out the inner diameter. We then drilled holes on the sides of the housing evenly so that the holes would line up with the blades in order to plug weld the stator inside of the housing. We machined a small lip so that the stator could sit inside of the housing before it was plug welded. The completed stator and stator housing assembly can be seen in Figure 21.



Figure 21: Stator and Stator Housing

3.11 Exhaust Nozzle

The primary function of an aircraft gas turbine exhaust nozzle is to generate thrust used to propel the aircraft forward (El-Sayed, 2015). This project focused on the design and manufacturing of a self-sustaining engine and we did not prioritize thrust. Our nozzle design objectives were to avoid choked flow and ensure ease of manufacturing. Therefore, we decided to choose a simple converging nozzle design derived from a popular RC jet turbine, the KJ-66. Our nozzle consists of a short outer cone with a 15-degree taper and a longer yet smaller in diameter inner cone. Additionally, we included eight tabs on the perimeter of the outer cone that

allow the nozzle to be bolted to the stator housing and outer casing. All of the components are manufactured from Inconel 718 sheet metal.

We used SolidWorks to create a model of the nozzle and generate a 2-dimensional template of the cones which we then transferred to a 0.02-in thick sheet of Inconel. We cut the sheet into two shapes, one for each cone, and tig welded them together. The outside cone was then bolted onto the casing using the tabs. The nozzle can be seen in Figure 20.



Figure 20: Nozzle

3.12 Bearings, Fuel Injection, and Lubrication

In order to build and operate an engine, it is essential to first consider the bearing, fuel, and lubrication that will keep rotating components moving efficiently. During the first stages of our design process we determined that it would not be feasible to design and build the ball bearings or the fuel and oil pumps. Through research regarding bearings used by RC jet modelers and manufacturers of small gas turbines, we identified a set of bearings that would be capable of withstanding the extreme temperatures and rotational speeds to be experienced in our engine. The bearings we chose are specifically offered, by BOCA Bearing, for miniature jet turbines, they are stainless steel/ceramic hybrid angular contact bearings capable of withstanding RPM up to 100,000 with proper lubrication.

Originally, the combustion chamber was designed specifically to accommodate liquid fuels through the use of the vaporization tubes. However, it became apparent later in the design process that we would be unable to purchase and assemble a fuel pump and throttle system within the allotted timeframe and budget. However, our engine is capable of running on multiple fuels, both liquid and gaseous. Therefore, we decided to run the engine on gaseous fuel in order to eliminate the need for a fuel pump and achieve throttling through the use of a valve. The theoretical minimal fuel consumption calculation using propane can be seen in Appendix C.

In order to ensure that the bearings would not fail at high rotational speeds and temperatures during operation, we incorporated a bearing lubrication system into our design. The system consists of two $\frac{1}{4}$ in stainless steel tubes entering

through the outer casing, running along the blackface of the diffuser, and entering the shaft housing at the location of each bearing. We also purchased an oil pump to push oil from a reservoir into the engine. The lubrication design can be seen in Figure 21.



Figure 21: Lubrication System

4.0 Conclusions and Recommendations

Over the course of this project we successfully designed and manufactured all twelve of the components outlined in Chapter 1 that constitute our jet engine. Additionally, we successfully assembled the engine. Figure 22 at the end of this section show the nozzle and compressor ends of the dry fit assembly. However, due to substantial manufacturing setbacks we were unable to test the engine before the deadline. These setbacks included the failed Inconel turbine and steel turbine asymmetry. In order to complete the manufacturing aspect of our project, we postponed our plans to manufacture a test stand, balance the shaft assembly, create a throttle mechanism, and seal the engine for operation.

In order to operate our engine by the end of this academic year, we plan to continue working towards creating the necessary components. We have contacted a local company specializing in balancing rotating components and they agreed to balance our shaft assembly. Creating a throttle mechanism for our engine has been simplified by the use of gaseous fuel. We plan to use an adjustable valve that controls the flow of propane therefore increasing or decreasing throttle. To ensure our engine is properly sealed, we will abandon the use of gasket paper and employ a high temperature silicon gasket sealer around the flange during final assembly. Finally, we plan to construct a simple static engine stand that will support the engine during operation and safeguard operators in the event of engine failure.

Despite our setbacks and failure to operate the engine in the given timeframe, we are working to complete the engine before the end of this academic year. In

order to provide assistance to any future project groups interested in manufacturing their own miniature gas turbine, we have provided a list of recommendations that will expedite the design and manufacturing process and possibly facilitate the integration of instrumentation, thrust considerations, and efficiency into their design.

- We recommend avoiding super alloys, like Inconel 718, when constructing a turbine unless the group has access to proper CNC tooling and equipment and experience machining with other similar alloys.
- We recommend that when selecting or manufacturing a compressor, ensure a CAD model is available. A CAD model enables the use of computer software to quickly design a compressor inlet shroud that meets tolerances necessary for engine efficiency.
- We recommend further research into flange design in order to create a flange that can integrate gasket material and ensure a proper, reliable seal.

Reflecting on the process we have gone through during the design and manufacturing of our engine has led us to realize the difficulties of designing and building an original engine. Many design advancements in gas turbines have been developed through experimentation and iteration. The design of any component manufactured during this project could be challenging enough to warrant a project of equal magnitude. Years of research and development could be spent designing a turbine blade or new combustion chamber. Additionally, the volume of research and information regarding gas turbines is simply immense and often difficult to

navigate. Considering these factors, it becomes evident that our project was quite ambitious. However, through our struggles, we gained first-hand knowledge of gas turbines and the challenges faced during their design and manufacturing.

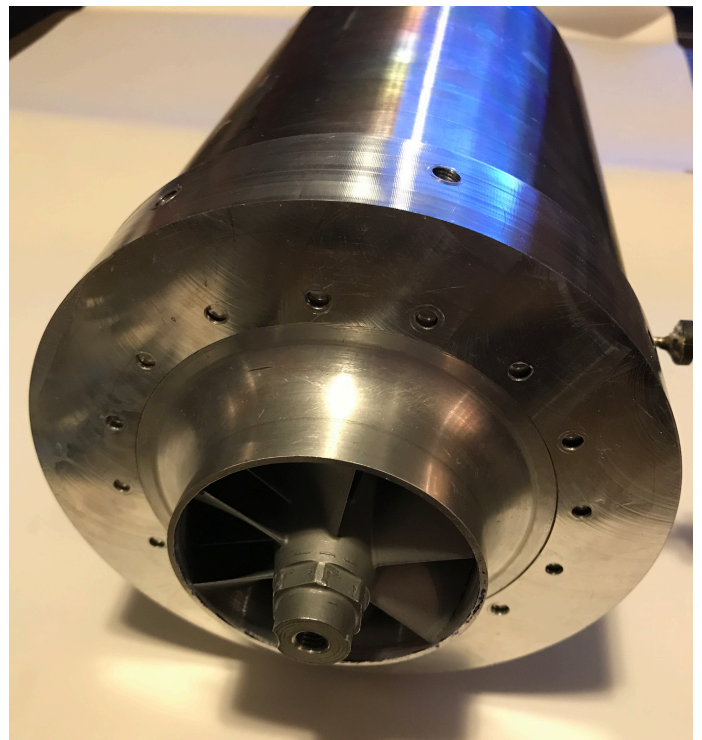


Figure 22: Nozzle (left) and Compressor (right) Views of Assembly

References

- Aviation. (2015, June 23). *Aviation*. Retrieved from Stack Exchange:
<https://aviation.stackexchange.com/questions/16177/what-are-the-differences-between-a-helicopter-engine-turboshaft-and-an-aircraft-engine>
- Benini, E., & Giacometti, S. (2007). Design, Manufacturing and Operation of a Small Turbojet-engine for Research Purposes. *Applied Energy*, 1102-1116.
- Boyce, M. P. (2012). *Gas Turbine Engineering Handbook (4th ed.)*. Amsterdam:Boston: Elsevier/Butterworth-Heinemann.
- Britannica, E. (2018). *Afterburner*. Retrieved from Encyclopedia Britannica :
<https://www.britannica.com/technology/afterburner-mechanical-engineering>
- Demirel, Y. (2012). *Energy: Production, Conversion, Storage, Conservation, and Coupling*. Lincoln, NE: Springer.
- El-Sayed, A. F. (2015). *Aircraft Propulsion and Gas Turbine Engines*. Boca Raton: CRC Press.
- Flack, R. (2005). *Fundamentals of Jet Propulsion with Applications*. Cambridge, UK: Cambridge University Press.
- Garret. (2017). *Compressor Maps*. Retrieved from Honeywell Garret:
https://www.turbobygarrett.com/turbobygarrett/compressor_maps
- Hill, P. G., & Peterson, C. R. (1992). *Mechanics and Thermodynamics of Propulsion*. Reading, MA: Addison-Wesley Pub. Co.
- Hunecke, K. (1997). *Jet Engines: Fundamentals of Theory Design and Operation*. Osceola, WI: Motorbooks International Publishers & Wholesalers.
- Kamps, T. (2005). *Model Jet Engines (3rd ed.)*. United Kingdom: Traplet Publications.
- Limit Engineering. (2015). *Garret Turbo Products GT4202*. Retrieved from Limit Engineering:
<http://www.limitengineering.com/Turbos/GT4202/GT4202.html>
- Ling, J., Wong, K., & Armfield, S. (2007). Numerical Investigation of a Small Gas Turbine Compressor. *16th Australasian Fluid Mechanics Conference* (pp. 961-966). Brisbane: School of Engineering, The University of Queensland.

- Macisaac, B., & Langton, R. (2011). *Gas Turbine Propulsion Systems*. Chichester, UK: Wiley.
- Mattingly, J. D. (2000). *Elements of Propulsion: Gas Turbines & Rockets*. American Institute of Aeronautics and Astronautics.
- MIT. (2014). *Applications of the First Law to Heat Engines*. Retrieved from MIT: http://web.mit.edu/16.unified/www/FALL/thermodynamics/chapter_5.htm
- Mukinutalapati, N. R. (2011). *Advances in Gas Turbine Technology*. InTech.
- NASA. (1973). *Design Handbook for Gaseous Fuel Engine Injectors and Combustion Chambers*. United States.
- NASA. (2015a, May 5). *Compressor*. Retrieved from NASA: <https://www.grc.nasa.gov/www/k-12/airplane/compress.html>
- NASA. (2015b, May 5). *Compressor Thermodynamics*. Retrieved from NASA: <https://www.grc.nasa.gov/www/k-12/airplane/compth.html>
- NASA. (2015c). *Turbojet Engine*. Retrieved from NASA: <http://www.grc.nasa.gov/www/k-12/airplane/aturbj.html>
- NASA. (2015d). *Turbine Thermodynamics*. Retrieved from NASA: <https://www.grc.nasa.gov/www/k-12/airplane/powtrbth.html>
- npower. (2009). *Forces on Large Steam Turbine Blades*. The Royal Academy of Engineering. RWE npower.
- Oates, G. C. (1997). *Aerothermodynamics of Gas Turbines and Rocket Propulsion*. Reston, VA: American Institute of Aeronautics and Astronautics.
- Shreckling, K. (1992). *Gas Turbines for Model Aircraft*. United Kingdom: Traplet Publications.
- Smith, C. W. (1956). *Aircraft Gas Turbines*. New York: John Wiley & Sons, Inc.
- Stricker, J. M. (1998). *The Gas Turbine Engine Conceptual Design Process - An Integrated Approach*. Wright-Patterson AFB, Air Force Research Laboratory.
- Thrust. (1985). *In Dictionary of Physics*. New York: Warner Books.
- Witkowski, T., White, S., Ortize Duenas, C., Strykowski, P., & Simon, T. (2003). *Characterizing the Performance of the SR-30 Turbojet Engine*. University of Minnesota.

APPENDIX A: Ideal Cycle Analysis

+. Ideal Turbojet Cycle Analysis

†The following values are based of of the Garrett GTX 4202 centrifugal compressor @ 85,000 rpm

$$\text{Molecular Weight of Air:} \quad M_a := 28.9645 \frac{\text{g}}{\text{mol}}$$

$$\text{Specific Gas Constant of Air:} \quad R_a := 287.058 \frac{\text{J}}{\text{kg} \cdot \text{K}}$$

$$\text{Freestream Mach number:} \quad M_0 := .01$$

$$\text{Freestream pressure:} \quad P_0 := 101325 \text{Pa}$$

$$\text{Freestream temperature:} \quad T_0 := 294 \text{K}$$

$$\text{Maximum temperature(turbine inlet):} \quad T_{t4} := 920 \text{K}$$

$$\text{Specific heat ratio at compressor:} \quad \gamma_c := 1.4$$

$$\text{Specific heat ratio at turbine:} \quad \gamma_t := 1.33$$

$$\text{Specific heat at compressor:} \quad C_{pc} := 1.005 \cdot 10^3 \frac{\text{N} \cdot \text{m}}{\text{kg} \cdot \text{K}}$$

$$\text{Specific heat at turbine:} \quad C_{pt} := 1.148 \cdot 10^3 \frac{\text{N} \cdot \text{m}}{\text{kg} \cdot \text{K}}$$

$$\text{Gas Constant at compressor:} \quad R_c := \frac{\gamma_c - 1}{\gamma_c} \cdot C_{pc} = 287.143 \frac{\text{m}^2}{\text{K} \cdot \text{s}^2}$$

Gas Constant at turbine:	$R_t := \frac{\gamma_t - 1}{\gamma_t} \cdot C_{pt} = 284.842 \frac{\text{m}^2}{\text{K} \cdot \text{s}^2}$
Compressor polytrophic efficiency:	$e_c := 0.78$
Turbine polytrophic efficiency:	$e_t := 0.74$
Freestream pressure ratio	$\pi_r := \left(1 + \frac{\gamma_c - 1}{2} \cdot M_0^2 \right)^{\frac{\gamma_c}{\gamma_c - 1}} = 1$
Freestream total pressure	$P_{t0} := \pi_r \cdot P_0 = 1.013 \times 10^5 \text{ Pa}$
Freestream temperature ratio	$\tau_r := 1 + \frac{\gamma_c - 1}{2} \cdot M_0^2 = 1$
Freestream total temperature	$T_{t0} := \tau_r \cdot T_0 = 294.006 \text{ K}$
Maximum stagnation enthalpy ratio	$\tau_\lambda := \frac{C_{pt} \cdot T_{t4}}{C_{pc} \cdot T_0} = 3.575$
Assumed total mass flow rate:	$m_a := 0.27 \frac{\text{kg}}{\text{s}}$

Inlet or Diffuser (1-2) :

Pressure Ratio:	$\pi_i := 1$
Pressure:	$P_{t2} := P_{t0} = 1.013 \times 10^5 \text{ Pa}$

Temperature Ratio: $\tau_i := 1$

Temperature: $T_{t2} := T_{t0} = 294.006 \text{ K}$

Compressor (2-3):

Pressure Ratio: $\pi_c := 3.2$

Pressure: $P_{t3} := P_{t2} \cdot \pi_c = 3.243 \times 10^5 \text{ Pa}$

Temperature Ratio: $\tau_c := (\pi_c)^{\frac{\gamma_c - 1}{\gamma_c \cdot e_c}} = 1.531$

Temperature: $T_{t3} := T_{t2} \cdot \tau_c = 450.187 \text{ K}$

Combustor or Burner (3-4) :

Pressure Ratio: $\pi_b := 1$

Pressure: $P_{t4} := P_{t3} \cdot \pi_b = 3.243 \times 10^5 \text{ Pa}$

Temperature Ratio: $\tau_b := \frac{T_{t4}}{T_{t3}} = 2.044$

Temperature: +

$$T_{t4} = 920 \text{ K}$$

Heat input:

$$Q_{in} := m_a \cdot C_{pc} \cdot (T_{t4} - T_{t3}) = 127.484 \text{ kW}$$

Turbine (4-5) :

Determine which pressure ratio yields optimal conditions.

Pressure Ratio:

$$\pi_t := 0.5$$

Pressure:

$$P_{t5} := \pi_t \cdot P_{t4} = 1.621 \times 10^5 \text{ Pa}$$

Temperature Ratio:

$$\tau_t := \pi_t^{\frac{\gamma_t}{\gamma_t - 1}} = 0.88$$

Temperature:

$$T_{t5} := \tau_t \cdot T_{t4} = 810.058 \text{ K}$$

Work output of turbine:

$$W_t := m_a \cdot C_{pt} \cdot (T_{t5} - T_{t4}) = -34.078 \text{ kW}$$

Nozzle (5-9) :

Pressure Ratio:

$$\pi_n := 1$$

Pressure:

$$P_{t9} := \pi_n \cdot P_{t5} = 1.621 \times 10^5 \text{ Pa}$$

Temperature Ratio:

$$\tau_n := 1$$

Temperature:

$$T_{t9} := \tau_n \cdot T_{t5} = 810.058 \text{ K}$$

Efficiencies :

Thermal Efficiency:

$$\eta_{th} := 1 - \frac{1}{\tau_r \cdot \tau_c} = 0.347$$

Propulsive Efficiency:

$$\eta_p := \frac{2 \cdot M_0}{\left[\frac{2 \cdot \tau_r}{\gamma_c - 1} \left(\frac{\tau_\lambda}{\tau_r \cdot \tau_c} - 1 \right) (\tau_c - 1) + \frac{\tau_\lambda}{\tau_r \cdot \tau_c} M_0^2 \right]^{\frac{1}{2}} + M_0} = 0.011$$

Overall Engine Efficiency:

$$\eta := \eta_{th} \cdot \eta_p = 3.666 \times 10^{-3}$$

Work :

Turbine Work:

$$m_a \cdot C_{pt} \cdot (T_{t4} - T_{t5}) = 34.078 \text{ kW}$$

Compressor Work:

$$W_c := m_a \cdot C_{pc} \cdot (T_{t3} - T_{t2}) = 42.38 \text{ kW}$$

$$\tau_T := \tau_i \cdot \tau_c \cdot \tau_t \cdot \tau_b = 2.755$$

$$a_o := \sqrt{\gamma_t \cdot R_a \cdot T_0} = 335.03 \frac{\text{m}}{\text{s}}$$

Mach Number At Exit:

$$M_e := \left(\frac{2}{\gamma_t - 1} \right)^{\frac{1}{2}} \cdot \left[\left(\frac{P_{t5}}{P_{t0}} \right)^{\frac{\gamma_t - 1}{\gamma_t}} - 1 \right]^{\frac{1}{2}} = 0.866$$

Speed of Sound:

$$s_s := 343 \frac{\text{m}}{\text{s}}$$

Thrust:

$$m_a \cdot M_e \cdot s = 80.183 \text{ N}$$

Appendix B: Turbine Blade Stress

Stress on Turbine Blades

+

Rotations per Minute:

$$N := 50000$$

Angular Velocity:

$$\omega := N \cdot 2 \frac{\pi}{60s} = 5.236 \times 10^3 \frac{\text{rad}}{\text{sec}}$$

Density of Steel:

$$\rho := 0.29 \frac{\text{lb}}{\text{in}^3} = 8.027 \times 10^3 \frac{\text{kg}}{\text{m}^3}$$

Youngs Modulus of Steel:

$$E := 28 \cdot 10^6 \text{ psi} = 1.931 \times 10^{11} \text{ Pa}$$

Outer Radius:

$$R_2 := 65.71 \frac{\text{mm}}{2} = 0.033 \text{ m}$$

Inner Radius:

$$R_1 := 11.42 \text{ mm} = 0.011 \text{ m}$$

Blade cross-sectional Area:

$$A := 67.93 \text{ mm}^2 = 6.793 \times 10^{-5} \text{ m}^2$$

Force :

$$F := (\rho \cdot A \cdot \omega^2) \frac{(R_2^2 - R_1^2)}{2} = 7.094 \times 10^3 \text{ N}$$

Blade root cross-sectional area:

$$A_{\text{root}} := A = 6.793 \times 10^{-5} \text{ m}^2$$

Blade Stress:

$$\sigma := \frac{F}{A_{\text{root}}} = 104.427 \text{ MPa}$$

Yield Strength (315 steel):

$$YS := 205 \text{ MPa}$$

Safety Factor:

$$SF := \frac{YS}{\sigma} = 1.963$$

Appendix C: Fuel Consumption Calculation

Fuel Consumption

Specific Heat of Air:
(at 800K)

$$C_p := 1100 \frac{\text{J}}{\text{kg} \cdot \text{K}}$$

Change in Temperature:
(Inlet - Exhaust)

$$\Delta T := 800 \text{K}$$

Assumed mass flow rate:

$$\dot{m} := 0.27 \frac{\text{kg}}{\text{s}}$$

Rate of Heat Transfer:

$$Q := \dot{m} \cdot C_p \cdot \Delta T = 0.238 \text{ MW}$$

Specific Energy of Propane:

$$\dot{e} := 50.3 \cdot 10^6 \frac{\text{J}}{\text{kg}}$$

Minimum fuel consumption :

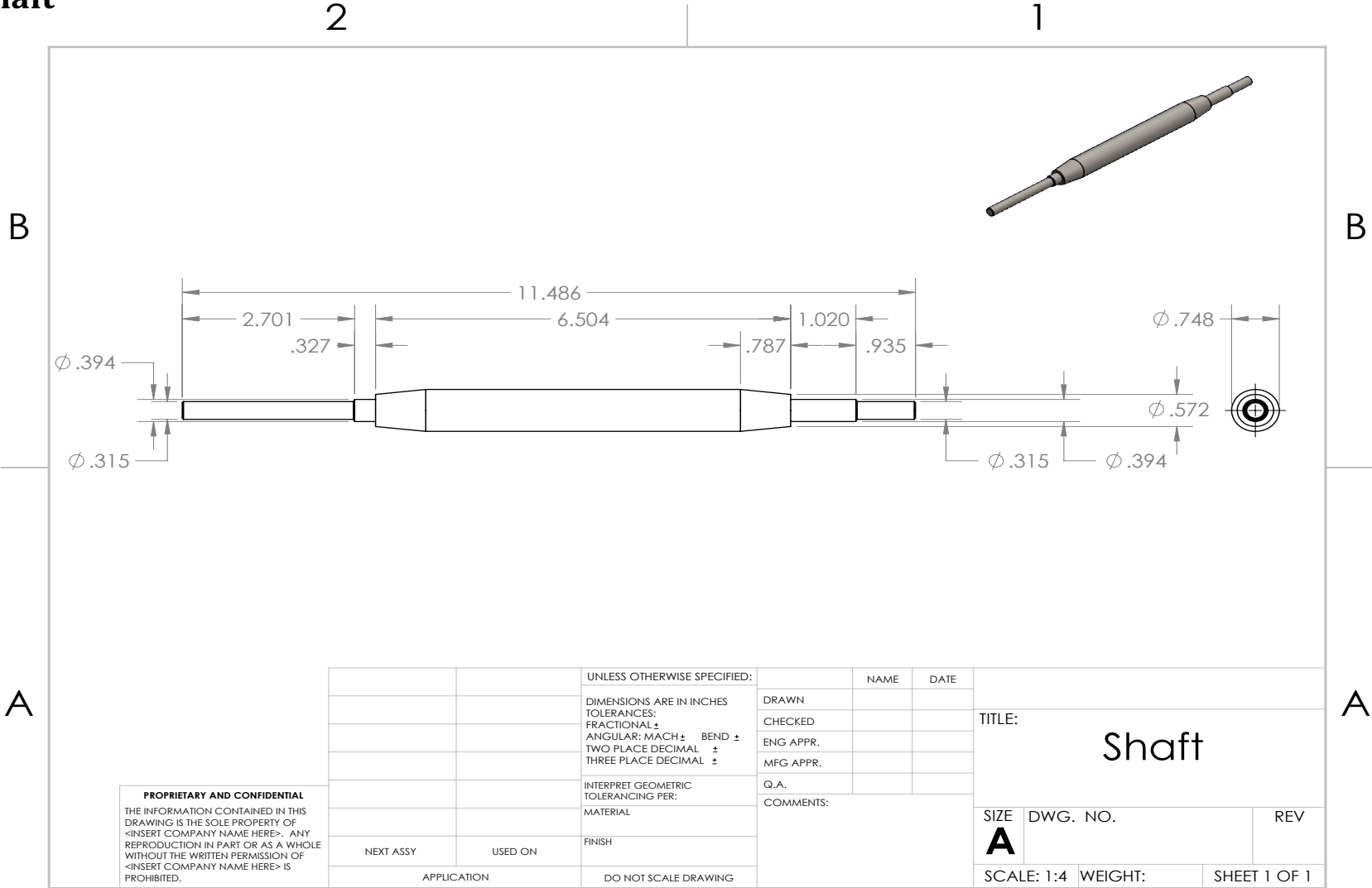
$$\dot{F} := \frac{Q}{\dot{e}} = 4.724 \times 10^{-3} \frac{\text{kg}}{\text{s}}$$

+

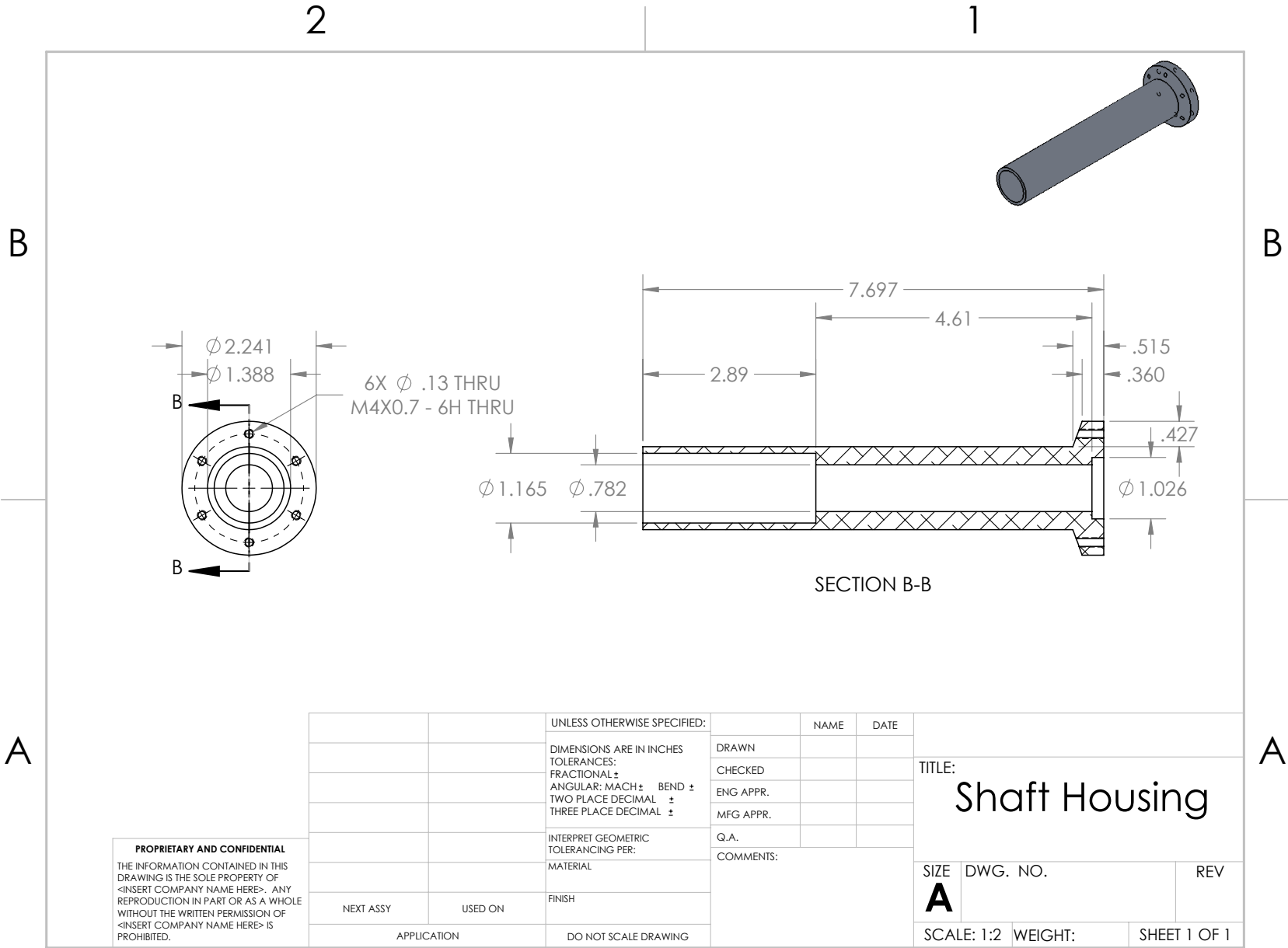
$$F_{\text{fuel}} := 4.724 \frac{\text{mL}}{\text{s}}$$

Appendix D: CAD Drawings

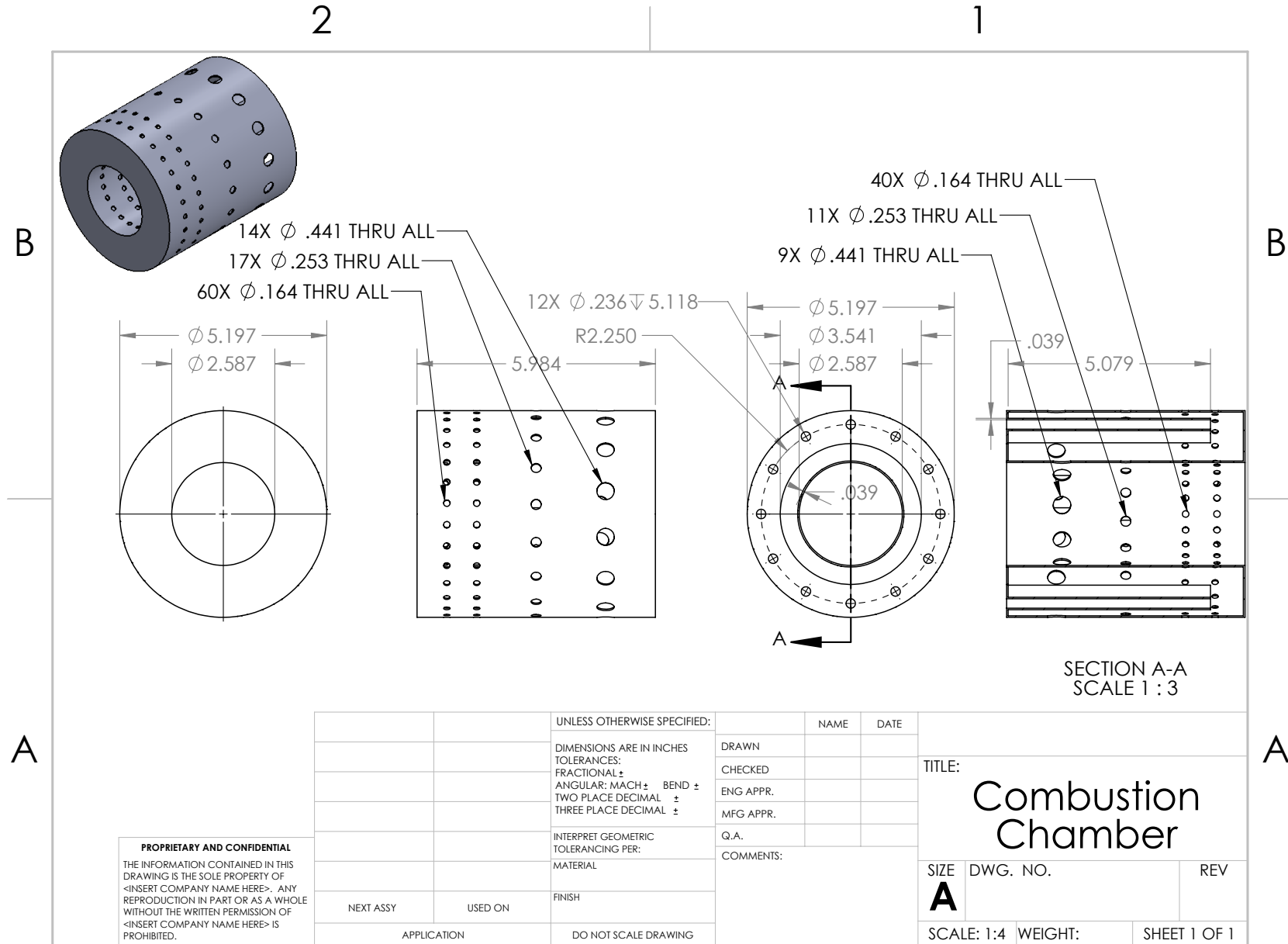
Shaft



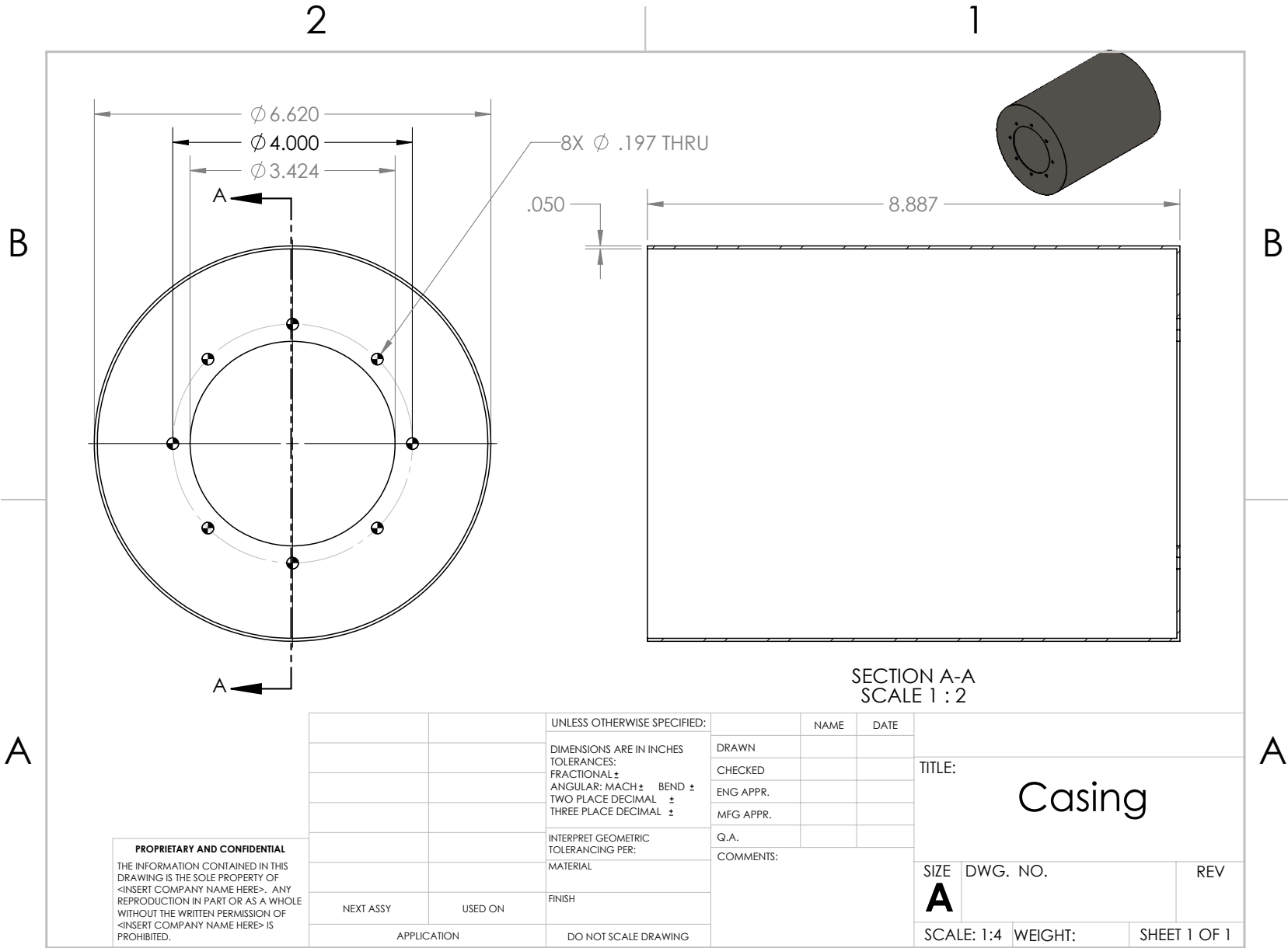
Shaft Housing



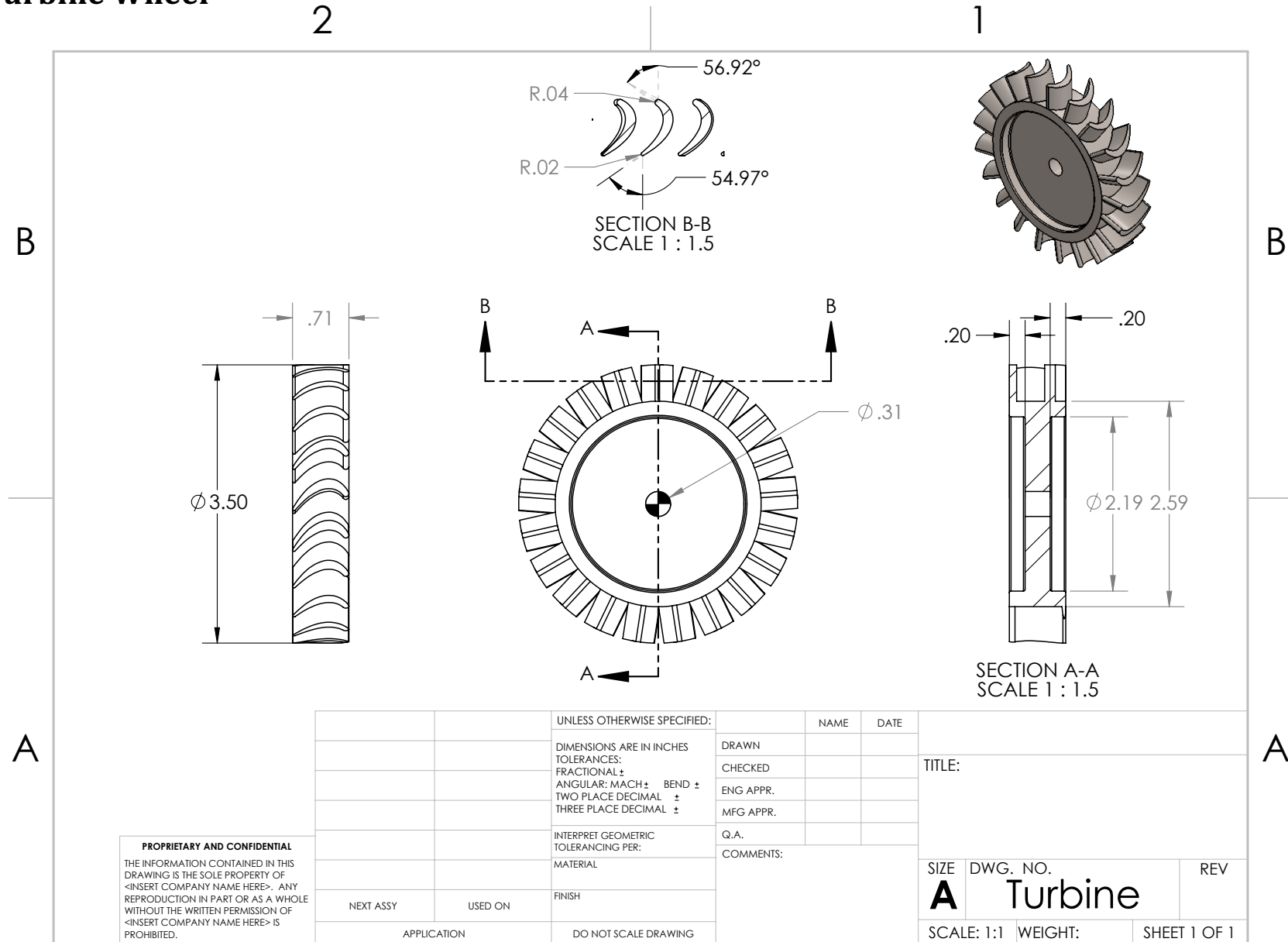
Combustion Chamber

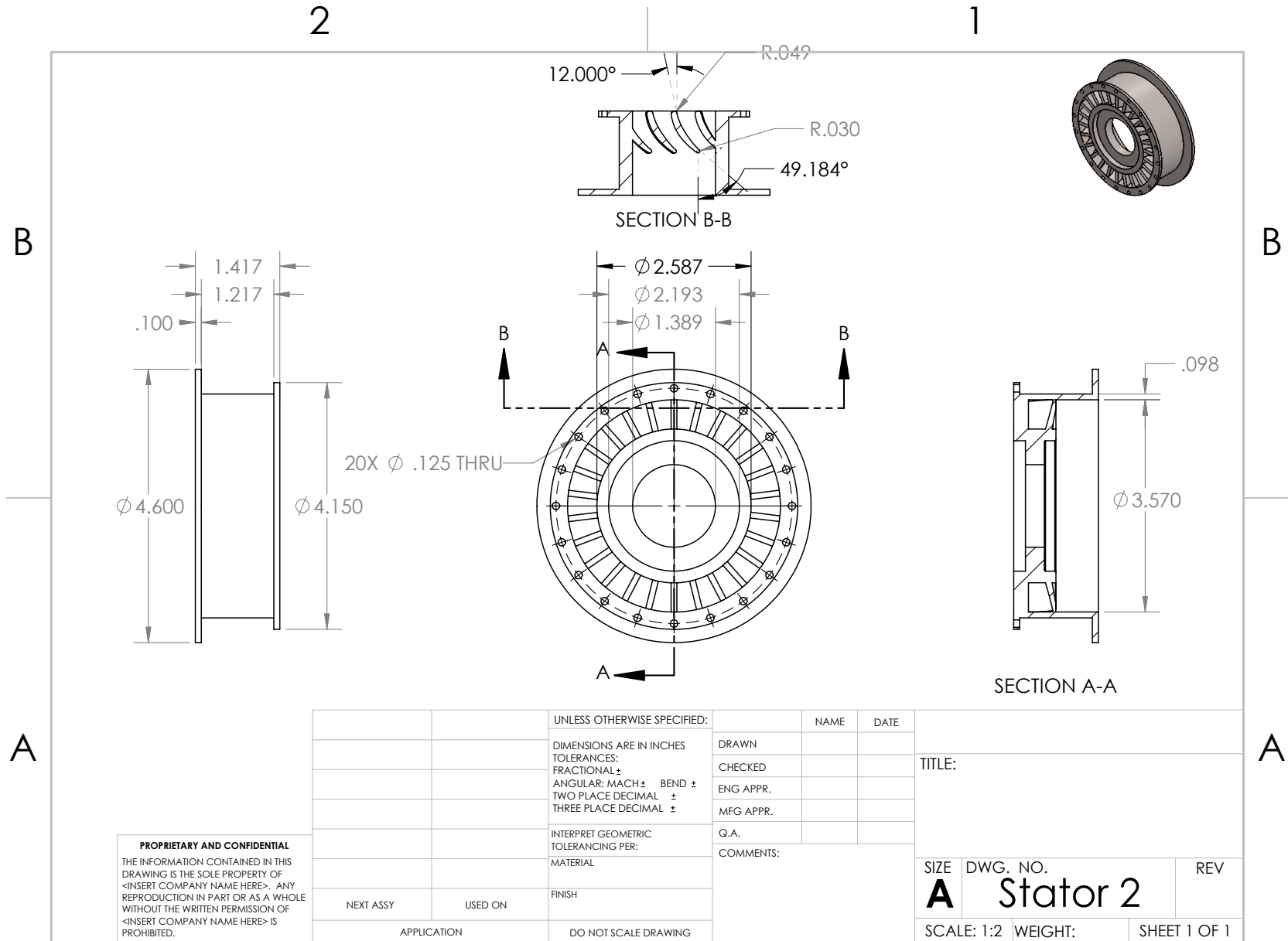


Outer Casing

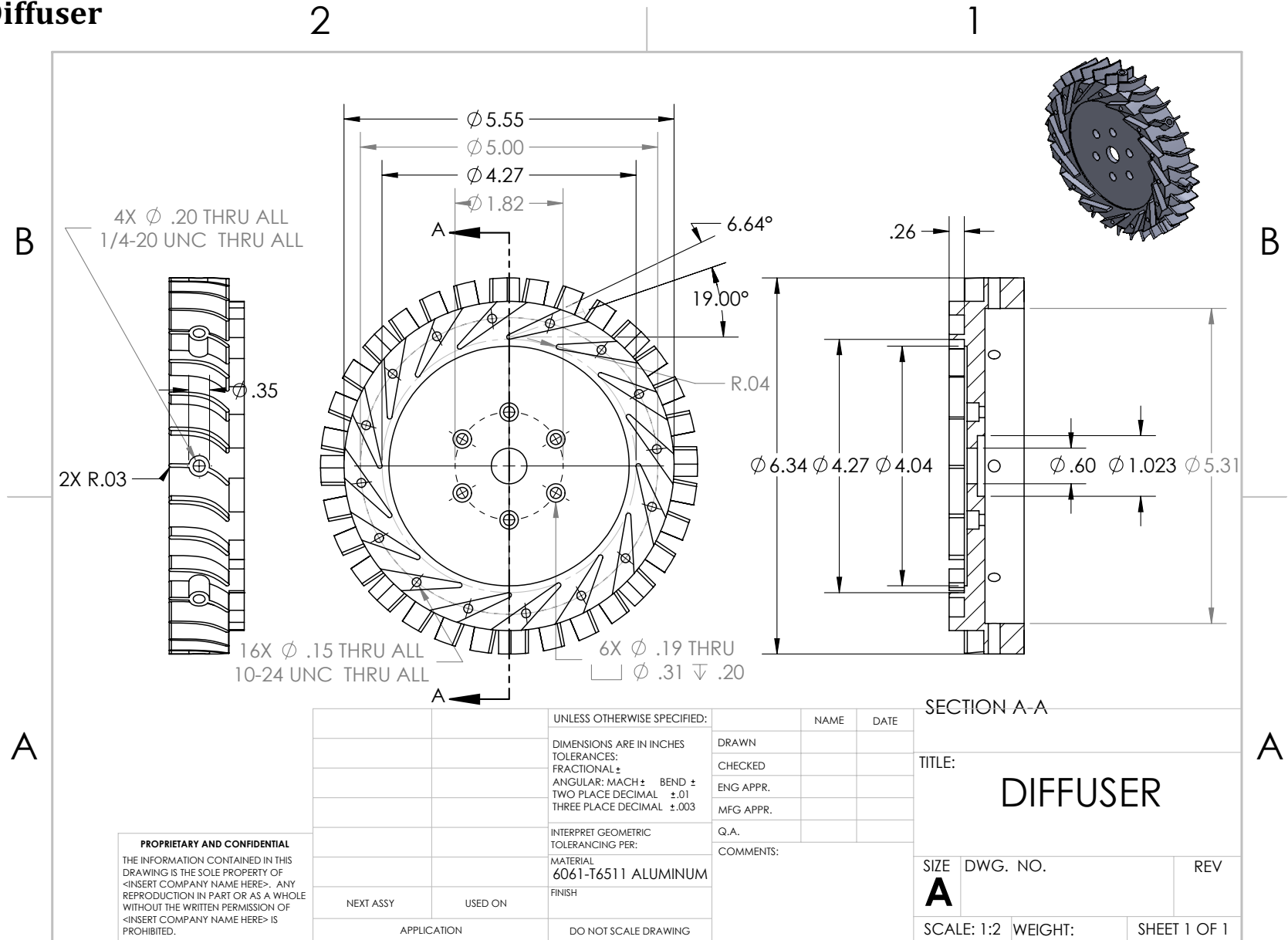


Turbine Wheel

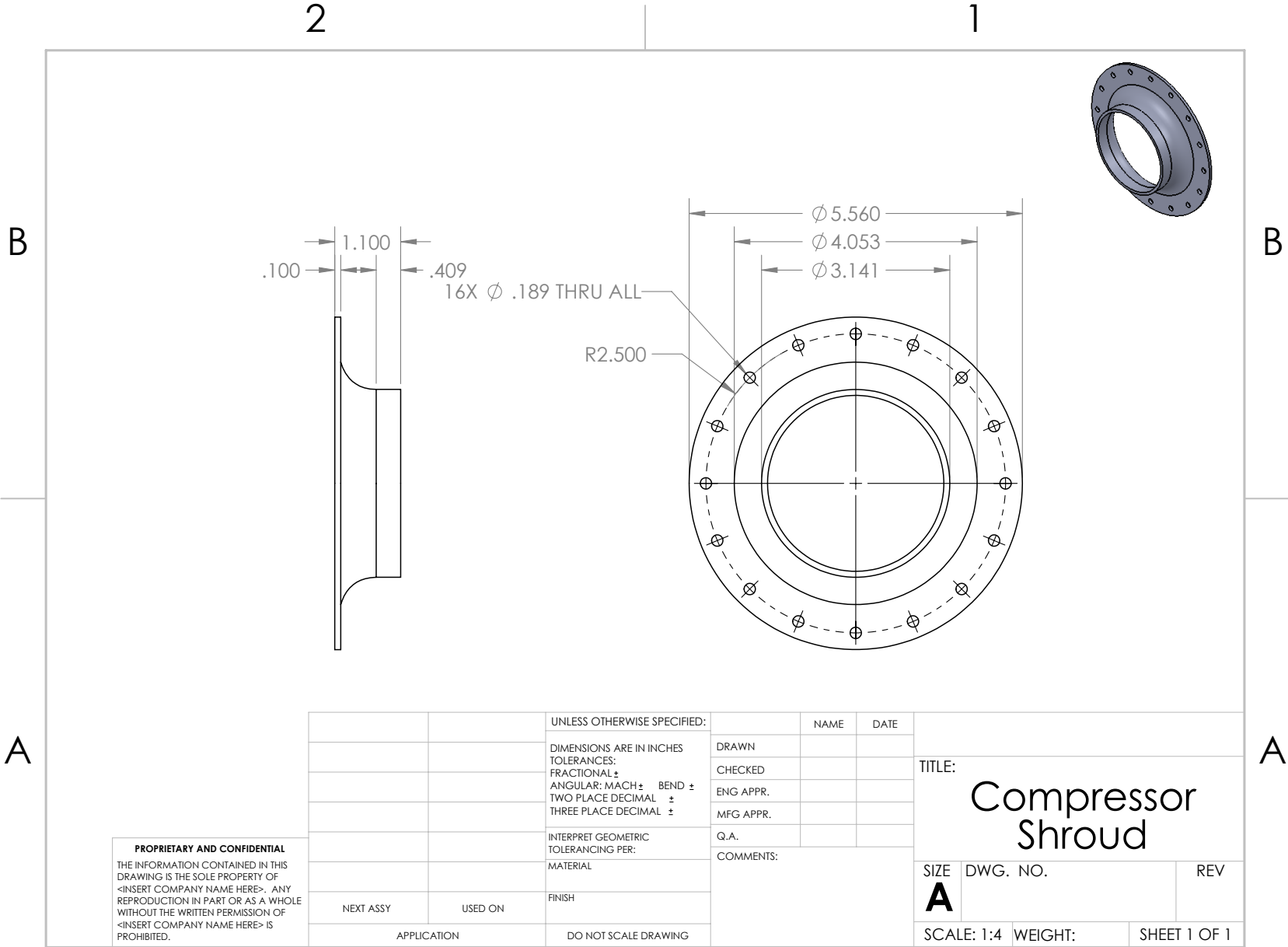


Stator & Stator Housing

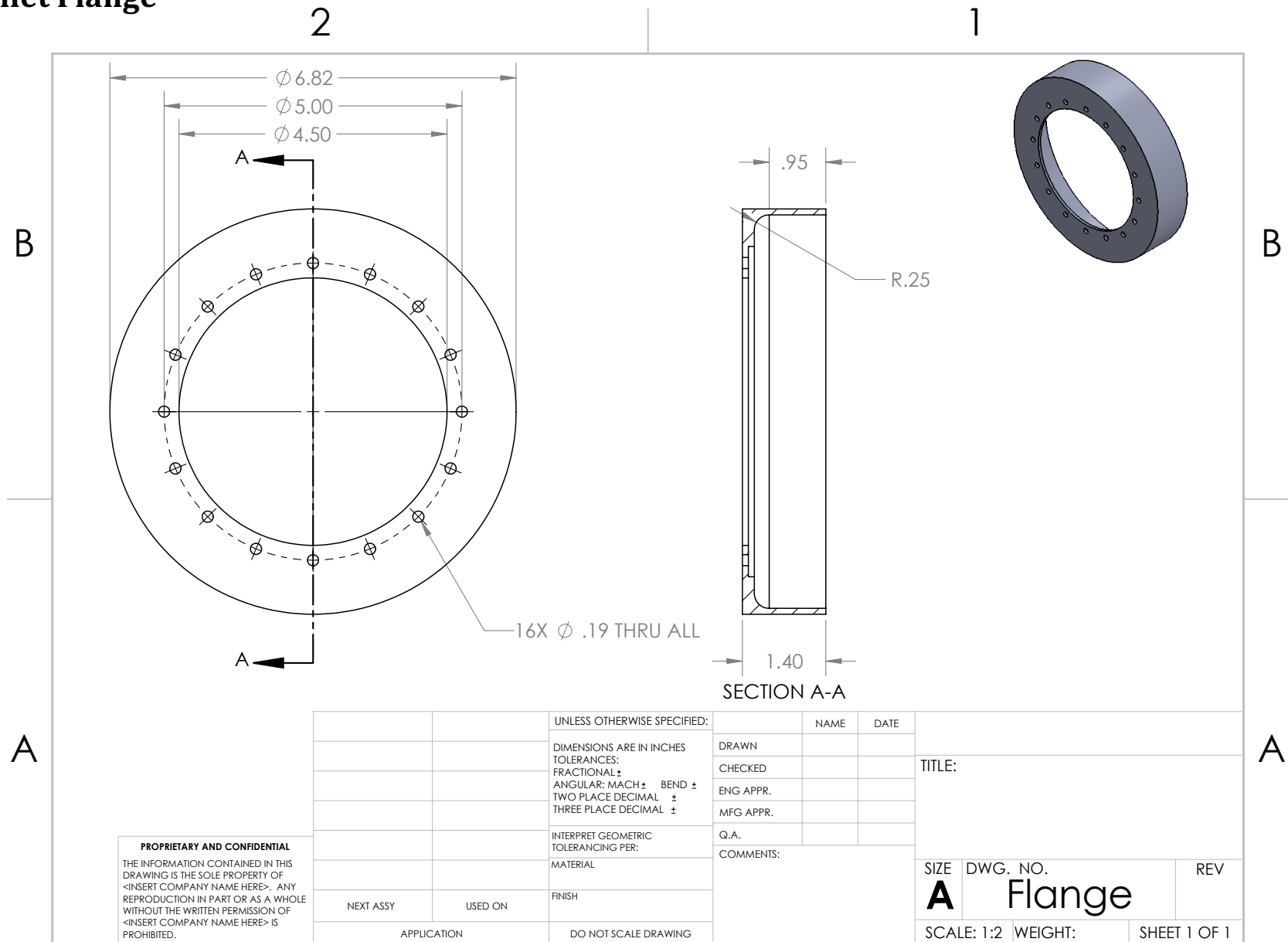
Diffuser



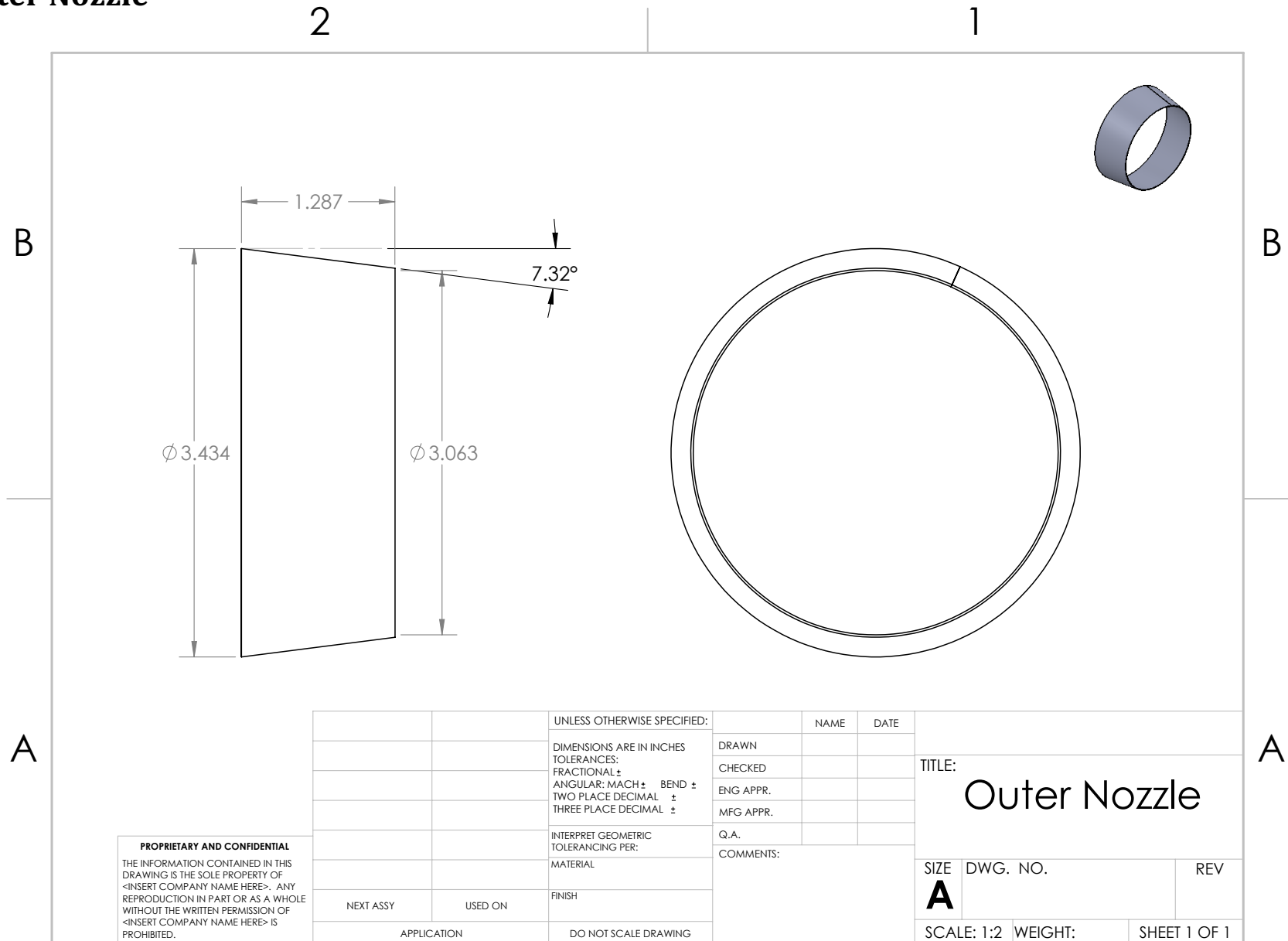
Compressor Shroud



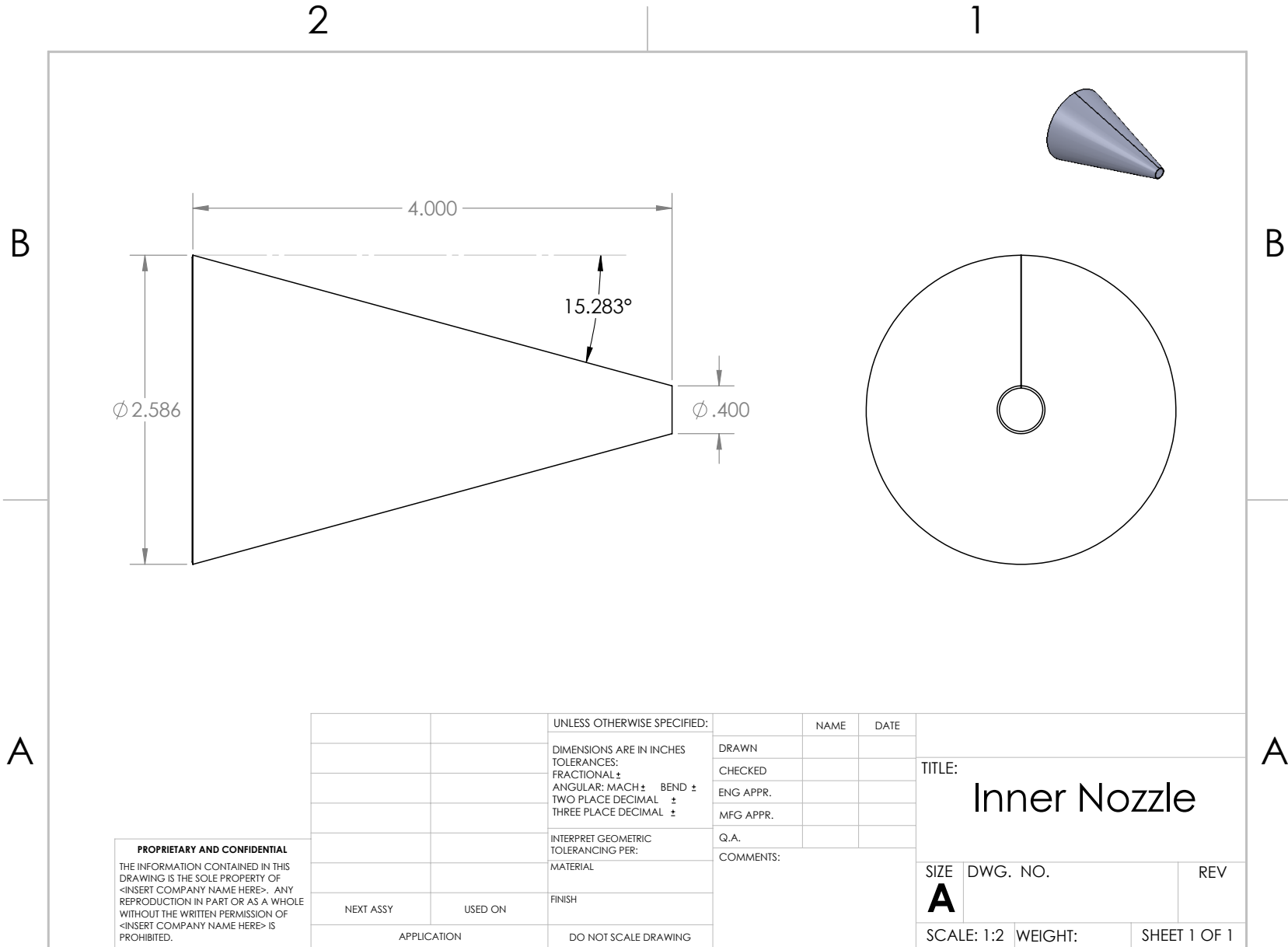
Inlet Flange



Outer Nozzle



Inner Nozzle



Engine Assembly

